AD-A058 769 ILLINOIS UNIV AT URBANA-CHAMPAIGN ELECTROMAGNETICS LAB F/G 20/14
PENETRATION OF AN EM WAVE INTO A CYLINDRICAL CAVITY AND THE CUR--ETC(U)
AUG 78 E K YUNG, S W LEE, R MITTRA N00014-75-C-0293
UNCLASSIFIED EM-78-9 NL

1 OF 1
AD A058 769

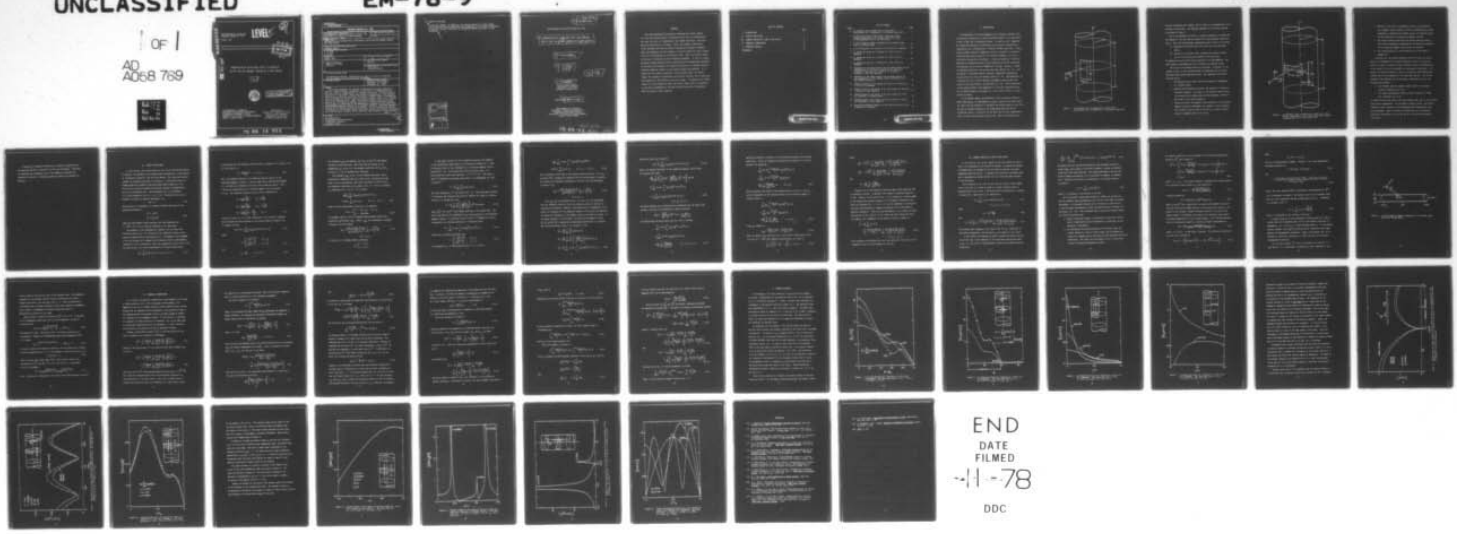

END
DATE FILMED
-11-78
DDC

ELECTROMAGNETICS LABORATORY
TECHNICAL REPORT NO. 78-9

August 1978

LEVEL II

PENETRATION OF AN EM WAVE INTO A CYLINDRICAL CAVITY AND THE CURRENT INDUCED ON A WIRE INSIDE

E. K. Yung
S. W. Lee
R. Mittra

ELECTROMAGNETICS LABORATORY
DEPARTMENT OF ELECTRICAL ENGINEERING
ENGINEERING EXPERIMENT STATION
UNIVERSITY OF ILLINOIS AT URBANA-CHAMPAIGN
URBANA, ILLINOIS 61801

Supported by
Contract No. N00014-75-C-0293
Office of Naval Research
Department of the Navy
Arlington, Virginia 22217

UNCLASSIFIED

Security Classification

DOCUMENT CONTROL DATA - R&D

(Security classification of title, body of abstract and indexing annotation must be entered when the overall report is classified)

1. ORIGINATING ACTIVITY (Corporate author)
Electromagnetics Laboratory, Dept. of Elec. Eng.
University of Illinois at Urbana-Champaign
Urbana, Illinois 61801

2a. REPORT SECURITY CLASSIFICATION

2b. GROUP

3. REPORT TITLE
PENETRATION OF AN EM WAVE INTO A CYLINDRICAL CAVITY AND THE CURRENT INDUCED ON A WIRE INSIDE

4. DESCRIPTIVE NOTES (Type of report and inclusive dates)
Technical Report

5. AUTHOR(S) (Last name, first name, initial)
E. K. Yung
S. W. Lee
R. Mittra

6. REPORT DATE
August, 1978

7a. TOTAL NO. OF PAGES
48

7b. NO. OF REFS
15

8a. CONTRACT OR GRANT NO.
N000 14-75-C-0293

b. PROJECT NO.

c.

d.

9a. ORIGINATOR'S REPORT NUMBER(S)
EM 78-9

9b. OTHER REPORT NO(S) (Any other numbers that may be assigned this report)
UILU-ENG-78-2551

10. AVAILABILITY/LIMITATION NOTICES

Distribution unlimited. Reproduction in whole or in part is permitted for any purpose of the United States Government.

11. SUPPLEMENTARY NOTES

12. SPONSORING MILITARY ACTIVITY
Office of Naval Research
Department of the Navy
Arlington, VA 22217

13. ABSTRACT

This paper addresses the problem of computing the current induced in a thin wire located inside a cylindrical cavity with a circumferential slot when the cavity is illuminated by an incident plane wave. The calculation is carried out in two steps. First, the problem of penetration of the incident field into the cavity is solved by the method of moments under the assumption that the presence of the wire inside the cavity creates little or no perturbation of the interior field. Next, the induced current on the wire is calculated by the following two methods: ~~(i)~~ use of a simple analytical formula derived from the application of the Wiener-Hopf techniques to the finite wire problem; and ~~(ii)~~ numerical solution of an integral equation. Extensive numerical results for the induced current are presented. It is found that the current is sensitive to the cylinder radius, the cavity height, the frequency of excitation, and the wire location, but is relatively less sensitive to the variation

(over)

14. KEY WORDS

EM Compatibility
Penetration through Apertures
Cylindrical Structure
Coupling to Wire

UNCLASSIFIED

Security Classification

Abstract Continued

in the slot length. In addition, the induced current on a wire inside the cavity can be much larger than its counterpart in free space illuminated by the same incident plane wave at frequencies where the cavity is near resonance.

(14) EM-78-9,
UILU-ENG-78-2551

Electromagnetics Laboratory Report No. 78-9

(6) PENETRATION OF AN EM WAVE INTO A CYLINDRICAL CAVITY AND THE CURRENT INDUCED ON A WIRE INSIDE.

(9) Technical Report,

(10) E. K. Yung,
S. W. Lee
R. Mittra

(12) 49p.

(11) August 1978

Office of Naval Research
Department of the Navy
Arlington, Virginia 22217

(15) Contract No. N00014-75-C-0293

Electromagnetics Laboratory
Department of Electrical Engineering
Engineering Experiment Station
University of Illinois at Urbana-Champaign
Urbana, Illinois 61801

ABSTRACT

This paper addresses the problem of computing the current induced in a thin wire located inside a cylindrical cavity with a circumferential slot when the cavity is illuminated by an incident plane wave. The calculation is carried out in two steps. First, the problem of penetration of the incident field into the cavity is solved by the method of moments under the assumption that the presence of the wire inside the cavity creates little or no perturbation of the interior field. Next, the induced current on the wire is calculated by the following two methods: (i) use of a simple analytical formula derived from the application of the Wiener-Hopf techniques to the finite wire problem; (ii) numerical solution of an integral equation. Extensive numerical results for the induced current are presented. It is found that the current is sensitive to the cylinder radius, the cavity height, the frequency of excitation, and the wire location, but is relatively less sensitive to the variation in the slot length. In addition, the induced current on a wire inside the cavity can be much larger than its counterpart in free space illuminated by the same incident plane wave at frequencies where the cavity is near resonance.

TABLE OF CONTENTS

LIST OF FIGURES

I. INTRODUCTION

The penetration of an electromagnetic wave through an aperture into a cylindrical structure is of current interest because of its application to EMP, to EMC, and to biological studies. As early as 1949, Sommerfeld [1] studied the problem of an infinitely long circular cylinder with a longitudinal slot, illuminated by a normally incident plane wave. Using a Fourier analysis approach, Sommerfeld reduced the problem to a system of infinitely many linear equations, but declared resignedly, "We can do practically nothing with the problem." Silver and Saunders [2] used the saddle-point integration method for the inversion of Fourier transforms and extracted the far field of Sommerfeld's problem. Hitherto, a number of extensions along this line of work have been reported [3], [4]. With the advent of high-speed digital computers, Sommerfeld's penetration problem can now be solved by numerical means [5], [6]. The penetration of an EM wave into the cylinder through a rectangular aperture was first carried out by Safavi-Naini, Lee and Mittra [7], [8]. Their problem has a more complex geometry than Sommerfeld's in that two conducting plates are introduced inside the cylinder at $z = \pm h$ to form a cavity, as illustrated in Figure 1.

In the present report, and extension of the penetration problem of Safavi-Naini *et al*. is investigated; in which a thin wire is added inside the cavity and the problem is to determine the current induced on the wire. The wire is oriented parallel to the longitudinal direction of the cylindrical cavity. If the slot in the cavity wall is also longitudinal, there is little induced current on the wire. Hence, we concentrate on

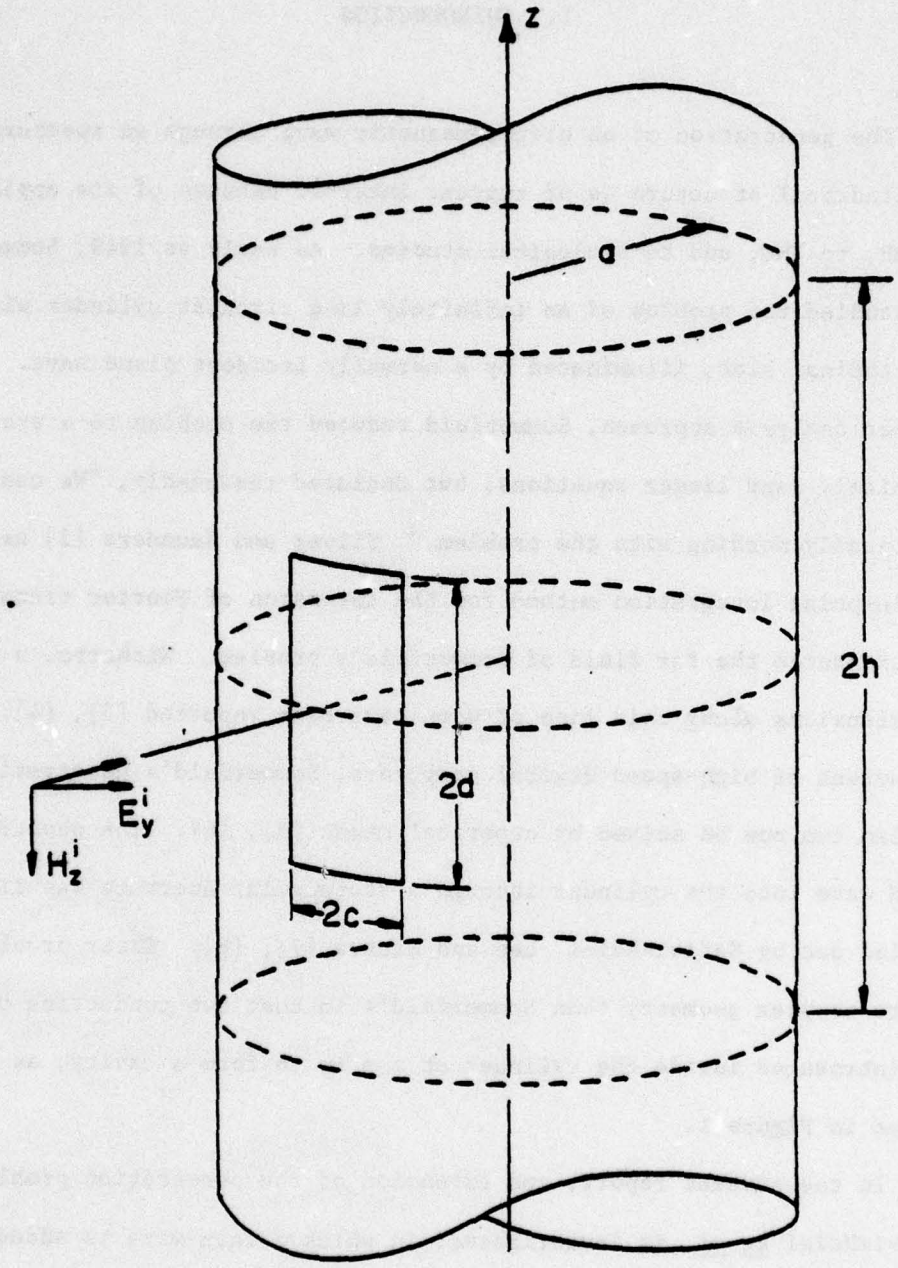

Figure 1. An infinitely long cylinder with a cavity and a longitudinal slot, illuminated by an incident plane wave.

the more interesting case, namely, the slot which is circumferential on the cylindrical cavity wall. The composite geometry of the present problem is sketched in Figure 2.

Due to the thinness of the wire, it appears reasonable to assume that the presence of the wire does not perturb the field generated inside the cavity. Thus, the problem under consideration can be solved in two steps:

(A) Determine the field $\overline{E}$ inside the cavity as if the wire were absent.

(B) Using $\overline{E}$ as an incident field, determine the induced current I(z) as if the wire were situated in the free space.

We emphasize that the above two-step approach is an approximation. The exact degree of approximation will be studied in a separate report.

The plan for the present report is as follows: In Section II, the problem of Part (A) with the wire absent is formulated and a system of infinitely many linear equations derived. The procedures are briefly described below:

1. The unknown electric field across the aperture is represented by a Fourier series.
2. Applying the equivalence principle, the aperture is shorted by a perfect conductor. The effect of the original aperture field is accounted for by introducing equivalent magnetic currents on both sides of the shorted aperture.
3. Inside the cavity, the magnetic field produced by the equivalent magnetic current is determined via a magnetic vector potential. The resultant field is given in the form of a doubly infinite series of eigenfunctions of the cavity.

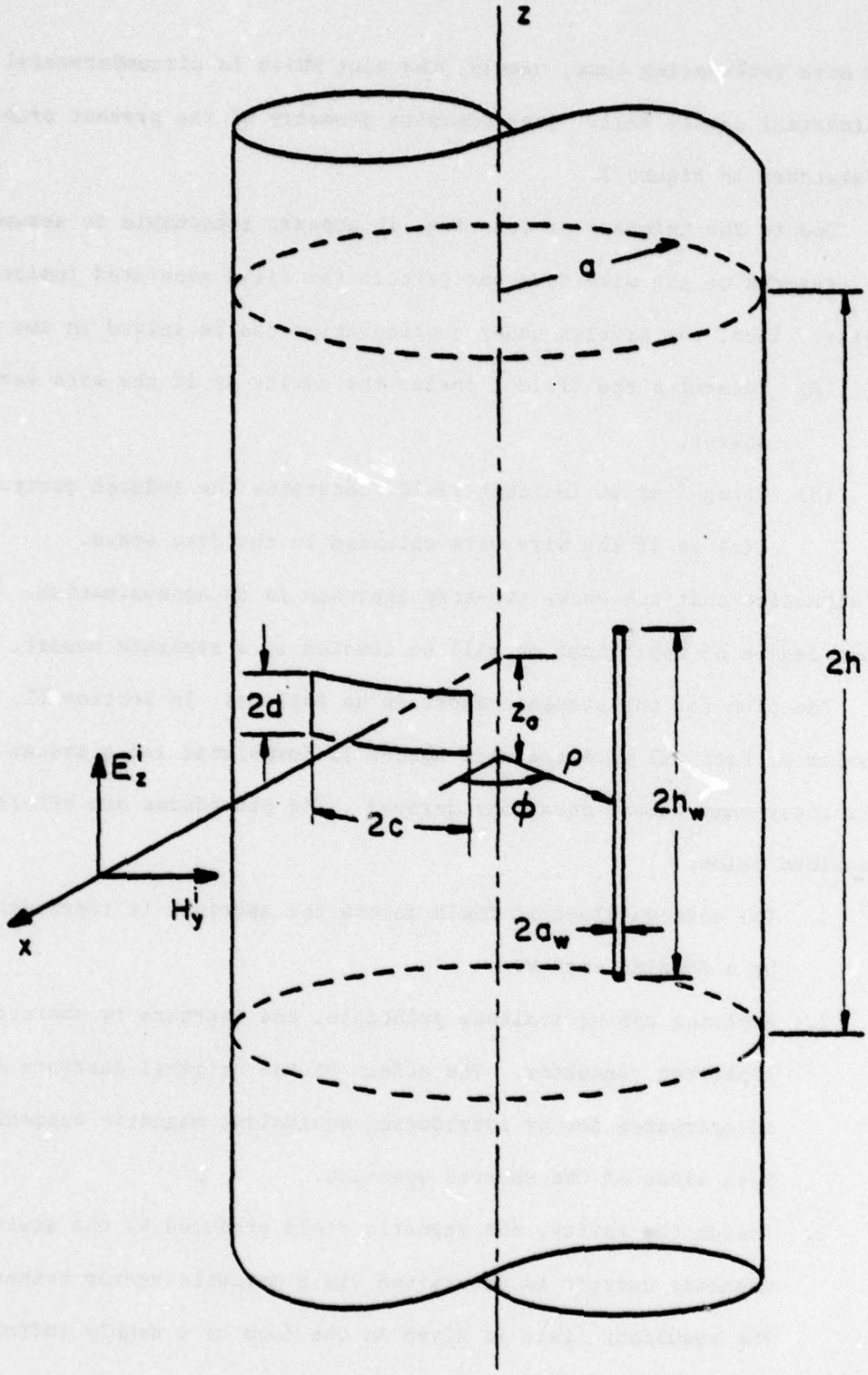

Figure 2. An infinitely long cylinder with a cavity and a wire inside, illuminated by an incident plane wave through a circumferential slot on the cavity wall.

4. Exterior to the cavity, the magnetic field is also generated via a magnetic vector potential, which is partitioned into three components to represent the incident field, the reflected field, and that produced by the equivalent magnetic current.
5. The coupled equation from which the unknown aperture electric field can be determined is developed by enforcing the continuity of the tangential magnetic field across the aperture.
6. The coupled equation is solved numerically by the method of moments [9].

In Section III, the current induced on the wire inside the cavity when it is illuminated by the field $\overline{E}$ computed in Part (A) is derived. Since $\overline{E}$ is given in terms of a doubly infinite series of eigenfunctions of the cavity, it can be interpreted as a spectrum of plane waves. As a result, the induced current I(z) can be determined by superimposing the currents due to each component of the plane wave spectrum. The current induced by each component of the spectrum is determined by one of the following two methods:

1. The standard numerical (moment) method based on an integral equation formulation [10], and
2. the simple approximation formula recently developed by Chang, Lee, and Rispin [11], [12].

It should be noted that both of the above methods apply only if the incident plane wave is homogeneous. In the present problem, however, the field $\overline{E}$ inside the cavity consists of both homogeneous and inhomogeneous plane wave components. Hence, the above two methods have to be extended by analytical continuation to cover the case of an incident inhomogeneous plane wave.

In Section IV, possible difficulties of numerical computations of the equations derived in Sections II and III are considered. Techniques for improving the convergence rate of the summation procedures are presented in Section IV. Extensive numerical results are presented in Section V.

II. FIELD IN THE CAVITY

In this section, the field $\bar{E}$ excited in the cavity with the wire absent is derived. The geometry of the problem under consideration in this section is illustrated in Figure 2, with the wire removed. The conducting circular cylinder is infinitely long and is of radius a. A cylindrical cavity is formed inside the cylinder by two conducting plates located at $z = \pm h$. The cavity is coupled to exterior excitations through a circumferential slot on its cylindrical wall. The rectangular slot is of dimension $2c \times 2d$ and centered at $(x = a, y = 0, z = 0)$. The width of the slot is assumed to be small in terms of wavelength, i.e.,

$$2kd << 1 \quad . \tag{2-1}$$

The structure is illuminated by a normally incident plane wave of unit magnitude described by

$$\begin{aligned} \bar{E}^i &= \hat{z}\, e^{ikx} \quad , \\ \bar{H}^i &= \hat{y}\, \frac{1}{\eta}\, e^{ikx} \end{aligned} \tag{2-2}$$

where the time harmonic factor $\exp(+j\omega t)$ has been suppressed and $\eta = \sqrt{\mu/\varepsilon} = 120\,\pi$ is the intrinsic impedance of the free space.

The symmetry of the configuration, together with the plane wave excitation given in Eq. 2-2, dictate that the tangential electric field across the aperture be an even function of ϕ. Furthermore, the narrowness of the slot enables us to assume that the aperture field is approximately constant in z and is z-directed. Thus, the tangential electric field across the aperture $\bar{E}_a = E_z \hat{z}$ can be represented by a Fourier-cosine series:

$$E_a = \sum_{\mu=0}^{\infty} E_\mu \cos \Gamma_\mu \phi; \quad |\phi| \leq \phi_0, \; |z| \leq d \quad . \tag{2-3}$$

In accordance with the boundary condition that E_a vanishes at $\phi = \pm\phi_0 (\phi_0 = c/a)$, $\{\Gamma_\mu\}$ are found to be

$$\Gamma_\mu = \frac{(2\mu + 1)\pi}{2\phi_0} \quad ; \mu = 0,1,2,\ldots \quad . \tag{2-4}$$

Due to the assumed direction of the aperture electric vector (or the equivalent magnetic current), it can be shown that a field TM with respect to z is sufficient torepresent the total field inside the cavity. Such a field can be generated via a z-directed magnetic vector potential $\bar{A} = A_z \hat{z}$. The relations between A_z and the field components are

$$E_\rho = \frac{1}{j\omega\mu\epsilon} \frac{\partial^2 A_z}{\partial\rho\partial z} \quad , \quad H_\rho = \frac{1}{\mu} \frac{\partial A_z}{\rho\partial\phi} \quad ,$$

$$E_\phi = \frac{1}{j\omega\mu\epsilon} \frac{\partial^2 A_z}{\rho\partial\phi\partial z} \quad , \quad H_\phi = -\frac{1}{\mu} \frac{\partial A_z}{\partial\rho} \quad ,$$

$$E_z = \frac{1}{j\omega\mu\epsilon}\left[\frac{\partial^2}{\partial z^2} + k^2\right]A_z \quad , \quad H_z = 0 \quad . \tag{2-5}$$

Inside the cavity, A_z is a linear combination of all possible elementary wave functions that are solutions to the scalar Helmholtz equation [13]. It assumes the form

$$A_z(\rho,\phi,z) = \sum_{m,n=0}^{\infty} A_{mn} J_m(\gamma_n\rho)\cos m\phi \cos \alpha_n z \tag{2-6}$$

where

$$\gamma_n = \begin{cases} \sqrt{k^2 - \alpha_n^2} & k^2 \geq \alpha_n^2 \quad , \\ -j\sqrt{\alpha_n^2 - k^2} \quad , & k^2 < \alpha_n^2 \quad , \end{cases} \tag{2-7}$$

and

$$\alpha_n = \frac{n\pi}{h} \quad , \quad n = 0,1,2,\ldots \tag{2-8}$$

The constants $\{A_{mn}\}$ are unknowns, and $\{J_m\}$ are the m^{th} order Bessel functions of the first kind. Note that with the choices of the eigenvalues $\{\alpha_n\}$ in Eq. 2-8, the boundary conditions that E_ρ and E_ϕ be zero at $z = \pm h$ are automatically satisfied.

The constants $\{A_{mn}\}$ in Eq. 2-6 are unknown quantities, and by enforcing the conditions that E_z be zero on the cylindrical wall and equal to E_a on the aperture, they can be evaluated in terms of $\{E_\mu\}$, the expansion coefficients of E_a given in Eq. 2-3. First, we evaluate E_z (referring to Eq. 2-5) at $\rho = a$ to obtain

$$\frac{1}{j\omega\mu\varepsilon} \sum_{m,n=0}^{\infty}\sum \gamma_n^2 A_{mn} J_m(\gamma_n a)\cos m\phi \cos \alpha_n z$$

$$= \Omega(\phi,z) \sum_{\mu=0}^{\infty} E_\mu \cos \Gamma_\mu \phi \quad ; \quad |\phi| \le \pi \ , \ |z| \le h \tag{2-9}$$

where Ω is the characteristic function of the aperture:

$$\Omega(\phi,z) = \begin{cases} 1 \ ; & |\phi| \le \phi_0 \ , \ |z| \le d \ , \\ 0 \ ; & \text{otherwise.} \end{cases} \tag{2.10}$$

We recognize that Eq. 2-9 is a standard Fourier-Bessel series with unresolved coefficients $\{A_{mn}\}$. Hence, $\{A_{mn}\}$ are determined by standard procedures with the results

$$A_{mn} = \frac{j4\omega\mu\varepsilon \cos m\phi_0 \sin \alpha_n d}{\varepsilon_m \varepsilon_n \pi \alpha_n \gamma_n^2 h J_m(\gamma_n a)} \sum_{\mu=0}^{\infty} E_\mu \frac{(-1)^\mu \Gamma_\mu}{\Gamma_\mu^2 - m^2} \tag{2-11}$$

$$m,n = 0,1,2,\ldots$$

in which ε_m is the Neumann number, defined by

$$\varepsilon_m = \begin{cases} 2 \ , & m = 0 \\ 1 \ , & m \neq 0 \end{cases} .$$

In the region exterior to the cylindrical structure, the symmetry of the configuration again leads to a TM field with respect to z. Thus, the exterior field is also determined via a z-directed magnetic vector potential $\overline{A}^{+} = \Psi\hat{z}$. For reasons which will be obvious later, Ψ is partitioned into three wave funcitons: $\Psi = \Psi^{i} + \Psi^{r} + \Psi^{s}$. The first of these Ψ^{i} represents the incident plane wave; it is independent of a and is given by

$$\Psi^{i} = \frac{j2}{\omega} \sum_{m=0}^{\infty} \frac{j^{m}}{\varepsilon_{m}} J_{m}(k\rho)\cos m\phi \quad . \tag{2-12}$$

The field components of Ψ^{i} are given in Eq. 2-2. The second wave function Ψ^{r} represents the reflected wave when the aperture is closed by a perfect conductor; it assumes the form:

$$\Psi^{r} = \frac{j2}{\omega} \sum_{m=0}^{\infty} \frac{j^{m}}{\varepsilon_{m}} \left\{ - \frac{J_{m}(ka)}{H_{m}^{(2)}(ka)} \right\} H_{m}^{(2)}(k\rho)\cos m\phi \tag{2-13}$$

where $\{H_{m}^{(2)}\}$ are the m^{th} order Hankel functions of the second kind. The third wave function Ψ^{s} corresponds to the field produced by the equivalent magnetic current. In contrast to both Ψ^{i} and Ψ^{r}, Ψ^{s} depends on a and is represented by a continuous spectrum of cylindrical waves:

$$\Psi^{s} = \sum_{m=0}^{\infty} \cos m\phi \int_{-\infty}^{\infty} F_{m}(\alpha) H_{m}^{(2)}(\gamma\rho) e^{j\alpha z} \, d\alpha \quad , \tag{2-14}$$

where $\{F_{m}\}$ are unknown functions, and

$$\gamma = \begin{cases} \sqrt{k^2 - \alpha^2} \quad , & k^2 \geq \alpha^2 \\ -j\sqrt{\alpha^2 - k^2} \quad , & k^2 < \alpha^2 \end{cases} \quad . \tag{2-15}$$

To determine $\{F_{m}\}$, we first evaluate E_{z}^{+} at $\rho = a$ to obtain

$$\frac{1}{j\omega\mu\varepsilon}\sum_{m=0}^{\infty}\cos m\phi\int_{-\infty}^{\infty}\gamma^2 F_m(\alpha)H_m^{(2)}(\gamma a)e^{j\alpha z}d\alpha$$

$$=\Omega(\phi,z)\sum_{\mu=0}^{\infty}E_\mu\cos\Gamma_\mu\phi\quad,\quad|\phi|\le\pi\quad,\quad|z|\le\infty\quad.\qquad(2\text{-}16)$$

Then, we multiply both sides of the equation above by cos $n\phi$, $n = 0,1,2,\ldots$, and after that, integrate the equation over the entire domain of interest. By invoking the orthogonal properties of $\{\cos n\phi\}$, $\{F_m\}$ are determined in terms of $\{E_\mu\}$:

$$F_m(\alpha)=\frac{j2\omega\mu\varepsilon\cos m\phi_0\sin\alpha d}{\varepsilon_m\pi^2\alpha\gamma^2H_m^{(2)}(\gamma a)}\sum_{\mu=0}^{\infty}E_\mu\frac{(-1)^\mu\Gamma_\mu}{\Gamma_\mu^2-m^2}\quad;\qquad(2\text{-}17)$$

$$m=0,1,2,\ldots\quad.$$

With $\{A_{mn}\}$ and $\{F_m\}$ defined by Eqs. 2-11 and 2-17, the requirement that the tangential electric field be continuous across the aperture is automatically satisfied. However, these definitions, of themselves, do not ensure the continuity of the tangential magnetic field across the aperture. To enforce the continuity of the magnetic field, we proceed as follows: In the region exterior to the cylinder, the three partial magnetic fields H_ϕ^i, H_ϕ^r, and H_ϕ^s (H_ρ^+ is immaterial) corresponding respectively to the three wave functions defined in Eqs. 2-12 through 2-14 are

$$H_\phi^i=\frac{2k}{j\omega\mu}\sum_{m=0}^{\infty}\frac{j^m}{\varepsilon_m}J_m'(k\rho)\cos m\phi\quad,$$

$$H_\phi^r=\frac{2k}{j\omega\mu}\sum_{m=0}^{\infty}\frac{j^m}{\varepsilon_m}\left[-\frac{J_m(ka)}{H_m^{(2)}(ka)}\right]H_m^{(2)\prime}(k\rho)\cos m\phi\quad,$$

$$H_\phi^s=\frac{-1}{\mu}\sum_{m=0}^{\infty}\cos m\phi\int_{-\infty}^{\infty}\gamma F_m(\alpha)H_m^{(2)\prime}(\gamma\rho)e^{j\alpha z}\,d\alpha\quad.\qquad(2\text{-}18)$$

Inside the cavity H_ϕ is given by

$$H_\phi = \frac{-1}{\mu} \sum_{m,n=0}^{\infty} \gamma_n A_{mn} J_m'(\gamma_n \rho) \cos m\phi \cos \alpha_n z \ . \qquad (2\text{-}19)$$

Hence, the desired continuity of the tangential magnetic field across the aperture now reads

$$\frac{2k}{j\omega\mu} \sum_{m=0}^{\infty} \frac{j^m}{\varepsilon_m} \left[J_m'(ka) - \frac{J_m(ka)}{H_m^{(2)}(ka)} H_m^{(2)'}(ka) \right] \cos m\phi$$

$$- \frac{1}{\mu} \sum_{m=0}^{\infty} \cos m\phi \int_{-\infty}^{\infty} \gamma F_m(\alpha) H_m^{(2)'}(\gamma a) e^{j\alpha z} \, d\alpha$$

$$= - \frac{1}{\mu} \sum_{m,n=0}^{\infty} \gamma_n A_{mn} J_m'(\gamma_n a) \cos m\phi \cos \alpha_n z \ ; \qquad (2\text{-}20)$$

$$|\phi| \le \phi_0, \ |z| \le d \ .$$

The above equation can be simplified by recognizing that the term in the bracket on the LHS is the Wronskian of Bessel functions:

$$J_m'(ka) - \frac{J_m(ka)}{H_m^{(2)}(ka)} H_m^{(2)'}(ka) = \frac{j2}{\pi ka H_m^{(2)}(ka)} \ .$$

By substituting the above result into Eq. 2-20, it becomes

$$\sum_{m=0}^{\infty} \cos m\phi \int_{-\infty}^{\infty} \gamma F_m(\alpha) H_m^{(2)'}(\gamma a) e^{j\alpha z} \, d\alpha$$

$$- \sum_{m,n=0}^{\infty} \cos m\phi \ \gamma_n A_{mn} J_m'(\gamma_n a) \cos \alpha_n z$$

$$= \frac{4}{\pi\omega a} \sum_{m=0}^{\infty} \frac{j^m \cos m\phi}{\varepsilon_m H_m^{(2)}(ka)} \quad ; \quad |\phi| \le \phi_{\hat{0}}, \ |z| \le d \ . \qquad (2\text{-}21)$$

Applying the method of Galerkin [9], the preceding equation can be solved numerically. First, we integrate the equation with respect to z over the aperture; the result is

$$\sum_{m=0}^{\infty} \cos m\phi \int_{-\infty}^{\infty} \frac{2 \sin \alpha d}{\alpha} \gamma F_m(\alpha) H_m^{(2)'}(\gamma a)\, d\alpha$$

$$- \sum_{m,n=0}^{\infty}\sum \cos m\phi \frac{2 \sin \alpha_n d}{\alpha_n} \gamma_n A_{mn} J_m'(\gamma_n a)$$

$$= \frac{4}{\pi\omega a} \sum_{m=0}^{\infty} \frac{j^m \cos m\phi}{\varepsilon_m H_m^{(2)}(ka)} 2d \quad ; \quad |\phi| \leq \phi_0 \ . \tag{2-22}$$

Next we multiply both sides of the equation above by $\cos \nu\phi$, $\nu = 0,1,2,\ldots$, and the integration of the resultant equation over the entire domain of interest leads to

$$\sum_{m=0}^{\infty} g_{m\nu} \int_{-\infty}^{\infty} \frac{\sin \alpha d}{\alpha} \gamma F_m(\alpha) H_m^{(2)'}(\gamma a)\, d\alpha$$

$$- \sum_{m,n=0}^{\infty}\sum g_{m\nu} \frac{\sin \alpha_n d}{\alpha_n} \gamma_n A_{mn} J_m'(\gamma_n a)$$

$$= \frac{4d}{\pi\omega a} \sum_{m=0}^{\infty} \frac{j^m}{\varepsilon_m} \frac{g_{m\nu}}{H_m^{(2)}(ka)} \quad ; \quad \nu = 0,1,2,\ldots, \tag{2-23}$$

where $g_{m\nu}$ stands for

$$g_{m\nu} = \frac{\sin(m-\nu)\phi_0}{m-\nu} + \frac{\sin(m+\nu)\phi_0}{m+\nu} \ . \tag{2-24}$$

Then, we replace $\{A_{mn}\}$ and $\{F_m\}$ in Eq. 2-23 by their definitions in Eqs. 2-11 and 2-17. After some algebraic manipulations, we arrive at

$$\sum_{\mu=0}^{\infty} E_\mu \left[\Lambda_{\mu\nu}^{(1)} + \Lambda_{\mu\nu}^{(2)} = D_\nu \right]; \quad \nu = 0,1,2,\ldots \tag{2-25}$$

where

$$\Lambda_{\mu\nu}^{(1)} = \frac{(-1)^{\mu}\Gamma_{\mu}}{\pi} \sum_{m=0}^{\infty} \frac{g_{m\nu}\cos m\phi_0}{\varepsilon_m(\Gamma_{\mu}^2 - m^2)} \int_0^{\infty} \frac{\sin^2 \alpha_n d \, H_m^{(2)'}(\gamma a)}{\alpha^2 \gamma \, H_m^{(2)}(\gamma a)} \, d\alpha \ ,$$

$$\Lambda_{\mu\nu}^{(2)} = -\frac{(-1)^{\mu}\Gamma_{\mu}}{h} \sum_{m=0}^{\infty} \frac{g_{m\nu}\cos m\phi_0}{\varepsilon_m(\Gamma_{\mu}^2 - m^2)} \sum_{n=0}^{\infty} \frac{\sin^2 \alpha_n d \, J_m'(\gamma_n a)}{\alpha_n^2 \gamma_n \, J_m(\gamma_n a)} \ ,$$

and

$$D_{\nu} = \frac{-jd}{k^2 a} \sum_{m=0}^{\infty} \frac{j^m g_{m\nu}}{\varepsilon_m H_m^{(2)}(ka)} \ .$$

Equation 2-25 is the system of infinitely many linear equations that we intended to derive. In general, this system of equations cannot be solved. However, if the series in Eq. 2-3 is truncated at a finite number N, the system would become a system of N x N algebraic equations, with which the unknowns $\{E_{\mu}\}$, $\mu = 0,1,2,\ldots N$, can be determined by solving the equations simultaneously by standard procedures such as the method of Gaussian elimination. After $\{E_{\mu}\}$ are determined, it is a matter of direct substitution of $\{E_{\mu}\}$ into Eq. 2-5 to obtain the field inside the cavity. For example, the z-component of the electric field E_z is given by

$$E_z = \frac{4}{\pi h} \sum_{\mu=0}^{\infty} E_{\mu}(-1)^{\mu}\Gamma_{\mu}$$

$$\times \sum_{n=0}^{\infty} \frac{\sin \alpha_n d \cos \alpha_n z}{\varepsilon_n \alpha_n} \sum_{m=0}^{\infty} \frac{\cos m\phi \cos m\phi_0 \, J_m(\gamma_n \rho)}{\varepsilon_m(\Gamma_{\mu}^2 - m^2) \, J_m(\gamma_n a)} \ ; \qquad (2\text{-}26)$$

$$\rho \leq a, \ |\phi| \leq \pi, \ |z| \leq h \ .$$

This completes our derivation for the field inside the cavity due to the incidence of Eq. 2-2 in the absence of the wire.

III. CURRENT INDUCED ON A WIRE IN THE CAVITY

In this section, the current induced on the wire inside the cavity when it is illuminated by the field $\bar{E}$ is derived. We attack the problem by assuming that the presence of the wire does not perturb the field generated inside the cavity. It enables us to use $\bar{E}$ as an incident field and to determine the induced current I(z) as if the wire were situated in the free space.

With reference to Eq. 2-26, we note that the electric field tangential to the wire E_z is given in terms of a doubly infinite series of eigenfunctions of the cavity. The series can be interpreted as a spectrum of plane waves. Explicitly, E_z is rewritten as

$$E_z = \sum_{n=-\infty}^{\infty} f_n(\rho,\phi) \exp(+jk \cos \theta_n z) \quad ; \tag{3-1}$$

$$\rho \leq a, \ |\phi| \leq \pi, \ |z| \leq h \quad ,$$

where

$$\theta_n = \cos^{-1}\left(\frac{n\pi}{kh}\right) \quad , \tag{3-2}$$

and

$$f_n = \frac{2}{\pi h} \sum_{\mu=0}^{\infty} E_\mu \frac{(-1)^\mu \Gamma_\mu \sin \alpha_n d}{\alpha_n} \sum_{m=0}^{\infty} \frac{\cos m\phi \cos m\phi_0 \ J_m(\gamma_n \rho)}{\epsilon_m(\Gamma_\mu^2 - m^2) \ J_m(\gamma_n a)} \quad . \tag{3-3}$$

We interpret each component of the field in Eq. 3-1 as a plane wave in free space propagating in the direction θ_n with respect to the z-axis.

In this report, two methods are used to compute the current induced on the wire due to each component of the plane wave spectrum described in Eq. 3-1. The first of these methods is based on an integral equation formulation:

$$\left(\frac{\partial^2}{\partial z^2} + k^2\right) \int_{z_0-h_w}^{z_0+h_w} I_n^{(1)}(z')K(z,z')dz' = -j4\pi\omega\varepsilon f_n e^{jk\cos\theta_n z} \quad . \quad (3\text{-}4)$$

The above thin wire scattering problem has been thoroughly studied in recent years, and a number of efficient programs to compute the unknown current $I_n^{(1)}$ have been developed. The program developed by Butler [10], which is based on solving Eq. 3-4 by the method of moments, is adopted here. Applying the principle of superposition, the induced current I is given by

$$I(z) = \sum_{n=-\infty}^{\infty} f_n(\rho,\phi) I_n^{(1)}(z) \quad , \quad (3\text{-}5)$$

where ρ is evaluated at the location of the wire.

As is well-known, using moment methods to compute the current on a wire is extremely time-consuming when the wire is of the order of several wavelengths. An alternative method that is suitable for long wires is to use the simple approximation formula developed recently by Chang, Lee and Rispin [11], [12]. The techniques used to derive this simple formula are briefly described below:

1. Using a Wiener-Hopf method, the reflection coefficient from the end of a semi-infinite wire illuminated by a plane wave of unit amplitude is determined.
2. By considering the multiple bounces of the current waves, the current induced on a wire of finite length can be expressed in terms of two Neumann series involving the just mentioned reflection coefficient. The series are then summed up into a closed form to give the desired approximation formula.

The induced current due to each component of the plane-wave spectrum is denoted by $I_n^{(2)}$ and is given by

$$I_n^{(2)}(z) = \left[C(\pi-\theta_n) \frac{R(\pi,h_w-z')}{R(\pi,2h_w)} + \Delta(\pi-\theta_n,h_w-z')\, V(\theta_n,h_w) \right] U(h_w-z')$$

$$+ \left[C(\theta_n) \frac{R(\pi,h_w+z')}{R(\pi,2h_w)} + \Delta(\theta_n,h_w+z')\, V(\pi-\theta_n,h_w) \right] U(h_w+z')$$

$$+ V(\theta_n,z') \quad , \tag{3-6}$$

where $z' = z - z_0$. In the above formula, V represents the current induced on an infinitely long cylinder by a unit plane wave:

$$V(\theta,z) = -\frac{j4\pi}{\eta} \frac{\exp(-jk\cos\theta_n z')}{\sin\theta_n\, W(k\cos\theta_n)} \quad , \tag{3-7}$$

in which W stands for

$$W = -j\pi J_0(ka_w \sin\theta_n) H_0^{(2)}(ka_w \sin\theta_n) \quad , \tag{3-8}$$

where J_0 and $H_0^{(2)}$ are, respectively, the zeroth-order Bessel function of the first kind and the Hankel function of the second kind, and a_w is the radius of the cylinder. Another universal function U is found in the simple formula; it represents the current on an infinitely long center-fed antenna generated by a unit voltage impulse. For a thin-wire antenna and for a sufficiently large kz, U can be accurately approximated by

$$U(z) \doteq \frac{2\pi}{\eta} \frac{\exp(-jk|z'|)}{\ell n(2k|z'|) - j\pi/2 - 2\ell n(ka_w) - \gamma} \quad , \tag{3-9}$$

where $\gamma = 0.57712...$ is the Euler's constant. The reflection coefficient R in Eq. 3-6 is defined by

$$R(\theta,z) = -\frac{\eta}{\pi}\left[\ell n(ka_w \sin\frac{\theta_n}{2}) + \gamma + j\frac{\pi}{2} + \frac{e^{jv_0}}{2} E_1(jv_0) \right] \quad , \tag{3-10}$$

where

$$V_\theta = kz'(1 - \cos\theta_n) \quad ,$$

and E_1 is the exponential integral. Finally, Δ and C are, respectively, shorthand notations for

$$\Delta = R(\theta_n, 2h_w) - R(\theta_n, h_w + z') \quad , \tag{3-11}$$

and

$$C = \frac{R(\pi-\theta_n, 2h_w)\, V(\theta_n, h_w) R(\pi, 2h_w)\, U(2h_w) - R(\theta_n, 2h_w)\, V(\pi-\theta_n, h_w)}{1 - [R(\pi, 2h_w)\, U(2h_w)]^2} \quad . \tag{3-12}$$

Again, the total induced current is obtained by superimposing all $I_n^{(2)}$. As is illustrated in Figure 3, the electric field of the incident plane wave is in the θ-direction and has an amplitude $f_n/\sin\theta_n$. Therefore, I is related to $I_n^{(2)}$ by

$$I(z) = \sum_{n=-\infty}^{\infty} f_n(\rho, \phi)\, \frac{I_n^{(2)}(z)}{\sin\theta_n} \quad , \tag{3-13}$$

where ρ is evaluated at the location of the wire.

A careful scrutiny of the techniques in deriving both $I_n^{(1)}$ and $I_n^{(2)}$ reveals that the two methods apply only if the incident plane wave is homogeneous, i.e., $\cos^2\theta_n \leq 1$ or real incident angle θ_n. In the present problem, however, the field $\bar{E}$ inside the cavity consists of both homogeneous and inhomogeneous components. Hence, both methods have to be extended by analytical continuation to cover the case of an incident inhomogeneous plane wave.

Let us first consider $I_n^{(1)}$ which is obtained by solving Eq. 3-4. Note that Eq. 3-4 is developed by equating the axial component of the

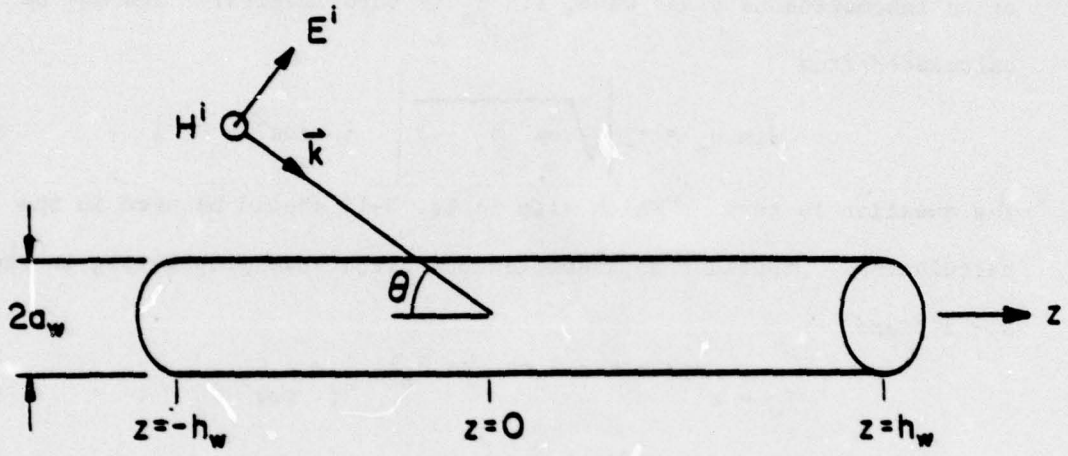

Figure 3. A finite length cylinder illuminated by an incident plane wave at an oblique angle.

electric field on the wire and that of the incident field. The tangential component of the incident electric field is $f_n \exp(+jk\cos\theta_n z)$ which remains valid even in the case when $\cos^2\theta_n > 1$. Thus no modification is necessary here, although allowances in the actual computer programming must be made to accommodate the rapidly oscillating nature of $\exp(+jk\cos\theta_n z)$ when $\cos\theta_n$ is large.

Next, we have to extend the formula of $I_n^{(2)}$ in Eq. 3-6. In the case of an inhomogeneous plane wave, $\sin\theta_n$ is pure imaginary, and may be calculated from

$$\sin\theta_n = \pm j\left|\sqrt{\cos^2\theta_n - 1}\right| \quad ; \quad \cos^2\theta_n > 1 \quad . \tag{3-14}$$

The question is then: "Which sign in Eq. 3-14 should be used in the calculation?" Consider an inhomogeneous plane wave propagating in the x - z plane:

$$E_y = e^{-jk(x\sin\theta_n + z\cos\theta_n)} \quad ; \quad \cos^2\theta_n > 1 \quad . \tag{3-15}$$

In order to satisfy the radiation condition, the field must decay (instead of grow) exponentially as $x \to +\infty$. This imposes a condition on $\sin\theta_n$, viz.,

$$I_m(\sin\theta_n) < 0. \tag{3-16}$$

Thus, the lower sign (minus sign) in Eq. (3-14) must be used in the calculation of $I_n^{(2)}$ from Eqs. 3-7, 3-8, 3-10, and 3-13. Furthermore, W in Eq. 3-8 becomes

$$W = 2I_0(ka_w\sqrt{\cos^2\theta_n - 1})K_0(ka_w\sqrt{\cos^2\theta_n - 1}) \quad , \tag{3-17}$$

where I_0 and K_0 are, respectively, the zeroth order modified Bessel functions.

IV. NUMERICAL COMPUTATIONS

As it stands, the numerical computation of each element of the system of linear equations in Eq. 2-25 is extremely time-consuming. The summation of the ratio of Bessel functions often presents another problem because both the numerator and the denominator could exceed the range of the computer and yet the quotient is still not small enough to warrant the termination of the summation process. In this section, a technique to circumvent the above difficulty is presented. And, at the same time, it significantly improves the rate of convergence. To best illustrate this technique, the evaluation of $\Lambda_{\mu\nu}^{(1)}$ is discussed in detail.

Besides a multiplying constant, $\Lambda_{\mu\nu}^{(1)}$ is rewritten below with the order of summation and integration interchanged:

$$\Lambda_{\mu\nu}^{(1)} = \int_0^\infty \frac{\sin^2 \alpha d}{\alpha^2 \gamma} \sum_{m=0}^{\infty} \frac{g_{m\nu} \cos m\phi_0}{\varepsilon_m (\Gamma_\mu^2 - m^2)} \frac{H_m^{(2)'}(\gamma a)}{H_m^{(2)}(\gamma a)} \, d\alpha \quad . \tag{4-1}$$

Because of the branch point $\alpha = k$, we partition the above integral into two parts:

$$\Lambda_{\mu\nu}^{(1)} = \int_0^k \frac{\sin^2 \alpha d}{\alpha^2 \gamma} \sum_{m=0}^{\infty} \frac{g_{m\nu} \cos m\phi_0}{\varepsilon_m (\Gamma_\mu^2 - m^2)} \frac{H_m^{(2)'}(\gamma a)}{H_m^{(2)}(\gamma a)} \, d\alpha$$

$$- \int_k^\infty \frac{\sin^2 \alpha d}{\alpha^2 \tau} \sum_{m=0}^{\infty} \frac{g_{m\nu} \cos m\phi_0}{\varepsilon_m (\Gamma_\mu^2 - m^2)} \frac{K_m'(\tau a)}{K_m(\tau a)} \, d\alpha \quad , \tag{4-2}$$

where $\{K_m\}$ are the m^{th} order modified Bessel functions and $\tau = \sqrt{\alpha^2 - k^2}$. Note that both integrands above have a non-integrable singularity in the neighborhood of the branch point. Hence, both integrals must be further partitioned such that the integration of a small region around

the branch point is deliberately isolated. Each of the partial integrals would be treated individually in the subsequent paragraphs.

The first integral to be treated is

$$I_1 = \int_0^{k-\delta} \frac{\sin^2 \alpha d}{\alpha^2 \gamma} \sum_H (\gamma a)\, d\alpha \quad , \tag{4-3}$$

where δ is an arbitrarily small number and $\sum_H$ represents the summation of Hankel functions. By invoking the recurrence relationship between the Hankel function and its derivative, $\sum_H$ becomes

$$\sum_H(u) = -G_{o\nu} \frac{H_1^{(2)}(u)}{H_0^{(2)}(u)} + \sum_{m=1}^{\infty} G_{m\nu} \left[\frac{H_{m-1}^{(2)}(u)}{H_m^{(2)}(u)} - \frac{m}{u} \right] \quad , \tag{4-4}$$

where $u = \gamma a$ and

$$G_{m\nu} = \frac{g_{m\nu} \cos m\phi_0}{\varepsilon_m (\Gamma_\mu^2 - m^2)} \quad ; \quad m = 0,1,2,\ldots \quad . \tag{4-5}$$

Since the real and imaginary parts of $\sum_H$ have different rates of convergence, they are treated independently as follows: First, by explicitly writing $H_m^{(2)}$ as $J_m + jY_m$, the real part of $\sum_H$ reads

$$\mathrm{Re}\{\sum_H\} = -G_{0\nu} \frac{J_0(u)J_1(u) + Y_0(u)Y_1(u)}{J_0^2(u) + Y_0^2(u)}$$

$$+ \sum_{m=1}^{\infty} G_{m\nu} \left[\frac{J_m(u)J_{m-1}(u) + Y_m(u)Y_{m-1}(u)}{J_m^2(u) + Y_m^2(u)} \right] . \tag{4-6}$$

Note that for a given u, the large-order approximations of each term of the sum can be extracted, which are

$$\lim_{m \to \infty} \left[\frac{J_m J_{m-1} + Y_m Y_{m-1}}{J_m^2 + Y_m^2} - \frac{m}{u} \right] = -\frac{m}{u} \tag{4-7}$$

and

$$\lim_{m\to\infty} G_{m\nu} = -\cos \nu\phi_0 \frac{\sin 2m\phi_0}{m^3} \quad . \tag{4-8}$$

By adding and subtracting the large-order approximations from each term of the sum, Eq. 4-6 becomes

$$\mathrm{Re}\{\Sigma_H\} = -G_{0\nu} \frac{J_0J_1 + Y_0Y_1}{J_0^2 + Y_0^2} + \sum_{m=1}^{\infty} \left\{ G_{m\nu} \left[\frac{J_mJ_{m-1} + Y_mY_{m-1}}{J_m^2 + Y_m^2} - \frac{m}{u} \right] - \frac{\cos \nu\phi_0}{u} \frac{\sin 2m\phi_0}{m^2} \right\} + \frac{\cos \nu\phi_0}{u} \sum_{m=1}^{\infty} \frac{\sin 2m\phi_0}{m^2} \quad . \tag{4-9}$$

The second sum can be evaluated analytically and the result is

$$\sum_{m=1}^{\infty} \frac{\sin 2m\phi_0}{m^2} = -\int_0^{2\phi_0} \ln(2 \sin \tfrac{t}{2})\, dt \quad . \tag{4-10}$$

The integral above is a thoroughly studied special function, known as Clausen's integral [14], whose value can be easily determined. The remaining sum in Eq. 4-9 has to be evaluated numerically. However, as compared with the sum in Eq. 4-6, which converges at a rate of m^{-2}, the modified sum converges at a much faster rate of m^{-4}. Furthermore, in evaluating the m^{th} order Bessel function B_m ($B_m = J_m$ or Y_m), we can apply the following recurrence formula:

$$B_{m+1}(u) = \frac{2m}{u} B_m(u) - B_{m-1}(u) \quad . \tag{4-11}$$

However, as is well-known, we should use this recurrence formula with extreme caution in computing J_m to avoid the so-called "propagation of error" when $2m/u > 1$. In the actual computation, the total sum is broken down into partial sums of 10, e.g., from n to n + 9. We first evaluate J_{n+4} and J_{n+5}; then, we apply the recurrence formula in both the forward and backward directions to obtain the rest of J_m. Moreover, we terminate

the summation by comparing the magnitude of the partial sum with the total sum. In doing so, we avoid the danger of terminating the summation prematurely in the case $2n\phi_0$ is a multiple of π (referring to Eq. 4-8).

As a final remark, when $ka_w >> 1$, $\sum_H$ can be approximated by

$$\sum_H(u) \doteq \frac{100}{u} \sum_H(u) \quad ; \quad u > 100 \quad . \tag{4-12}$$

On the other hand, no modification is necessary to sum $\mathrm{Im}\{\sum_H\}$ because its large-order approximation is zero.

The second integral of concern is

$$I_2 = \int_{k+\delta}^{\infty} \frac{\sin^2 \alpha d}{\alpha^2 \tau} \sum_K(\tau a)\, d\alpha \quad , \tag{4-13}$$

where $\sum_K$ represents the summation of the modified Bessel functions $\{K_m\}$. With the derivative of K_m written in terms of K_m and K_{m-1}, $\sum_K$ reads

$$\sum_K(v) = - G_{0\nu} \frac{K_1(v)}{K_0(v)} - \sum_{m=1}^{\infty} G_{m\nu} \left[\frac{K_{m-1}(v)}{K_m(v)} + \frac{m}{v} \right] \quad , \tag{4-14}$$

in which $v = \tau a$. Since the large-order approximation of each term of the sum is

$$\lim_{m \to \infty} \left[\frac{K_{m-1}(v)}{K_m(v)} + \frac{m}{v} \right] = \frac{m}{v} \quad , \tag{4-15}$$

we evaluate $\sum_K$ as

$$\sum_K = - G_{0\nu} \frac{K_1(v)}{K_0(v)} + \frac{\cos \nu\phi_0}{v} \sum_{m=1}^{\infty} \frac{\sin 2m\phi_0}{m^2}$$

$$- \sum_{m=1}^{\infty} \left\{ G_{m\nu} \left[\frac{K_{m-1}}{K_m} + \frac{m}{v} \right] + \frac{\cos \nu\phi_0}{v} \frac{\sin 2m\phi_0}{m^2} \right\} \quad . \tag{4-16}$$

The above formula is similar to Eq. 4-9; therefore, it is evaluated by similar techniques. Furthermore, we extract the large argument approximation

of $\sum_K$, which is

$$\sum_K(v) \doteq \sum_K(150) \quad ; \quad v \geq 150 \quad . \tag{4-17}$$

Substituting the results of Eqs. 4-16 and 4-17 into Eq. 4-13, we arrive at

$$I_2 = \int_{k+\delta}^{\pi/d} \frac{\sin^2 \alpha d}{\alpha^2 \tau} \sum_K(\tau a)\, d\alpha + \sum_{n=1}^{\infty} \int_{n\pi/d}^{(n+1)\pi/d} \frac{\sin^2 \alpha d}{\alpha^2} \left[\frac{1}{\tau} \sum_K(\tau a) - \frac{1}{\alpha} \sum_K(150) \right] d\alpha + \sum_K(150) \int_{\pi/d}^{\infty} \frac{\sin^2 \alpha d}{\alpha^3}\, d\alpha \quad . \tag{4-18}$$

By two successive integrations by parts, the last integral above is transformed into

$$\int_{\pi/d}^{\infty} \frac{\sin^2 \alpha d}{\alpha^3}\, d\alpha = d^2 \int_{2\pi}^{\infty} \frac{\cos t}{t}\, dt = - d^2 C_i(2\pi) \quad , \tag{4-19}$$

where C_i is the cosine integral [15].

The third integral of concern is

$$I_3 = \int_{k-\delta}^{k} \frac{\sin^2 \alpha d}{\alpha^2 \gamma} \sum_H(\gamma a)\, d\alpha - \int_{k}^{k+\delta} \frac{\sin^2 \alpha d}{\alpha^2 \tau} \sum_K(\tau a)\, d\alpha \quad . \tag{4-20}$$

First, we examine the small-argument behaviors of both $\sum_H$ and $\sum_K$; they are

$$\lim_{u \to 0} \mathrm{Re}\{\sum_H\} = - \frac{1}{u} \sum_{m=1}^{\infty} m G_{m\nu} \quad ,$$

$$\lim_{u \to 0} I_m\{\sum_H\} = - \frac{\pi G_{o\nu}}{2u \ell n^2 u} \quad ,$$

and

$$\lim_{v \to 0} \sum_K = - \frac{1}{v} \sum_{m=1}^{\infty} m G_{m\nu} \quad . \tag{4-21}$$

It can be easily shown that the real part of I_3 tends to zero, and its imaginary part can be approximated by

$$I_m\{I_3\} = \frac{\pi G_{0\nu} \sin^2 kd}{2ak^3 \ell n(a\sqrt{2k\delta})} \quad . \tag{4-22}$$

Since the forms of $\Lambda_{\mu\nu}^{(1)}$ and $\Lambda_{\mu\nu}^{(2)}$ are similar, analogous techniques are employed to evaluate $\Lambda_{\mu\nu}^{(2)}$; the result is (besides a multiplying constant)

$$\Lambda_{\mu\nu}^{(2)} = \sum_{n=0}^{N} \frac{\sin^2 \alpha_n d}{\varepsilon_n \alpha_n^2 \gamma_n} \zeta_J(\gamma_n a) - \sum_{n=N+1}^{\infty} \frac{\sin^2 \alpha_n d}{\alpha_n^2} \left[\frac{1}{\tau_n} \zeta_I(\tau_n a) - \frac{1}{\alpha_n} \zeta_I(150) \right]$$

$$- \left(\frac{h}{\pi}\right)^3 \zeta_I(150) \sum_{n=N+1}^{\infty} \frac{\sin^2 \alpha_n d}{n^3} \quad , \tag{4-23}$$

where N = Integer (kh/π) and

$$\zeta_J(u) = - G_{0\nu} \frac{J_1(u)}{J_0(u)} - \frac{\cos \nu\phi_0}{u} \sum_{m=1}^{\infty} \frac{\sin 2m\phi_0}{m^2}$$

$$+ \sum_{m=1}^{\infty} \left\{ G_{m\nu} \left[\frac{J_{m-1}(u)}{J_m(u)} - \frac{m}{u} \right] + \frac{\cos \nu\phi_0}{u} \frac{\sin 2m\phi_0}{m^2} \right\}, \tag{4-24}$$

and

$$\zeta_I(u) = G_{0\nu} \frac{I_1(u)}{I_0(u)} - \frac{\cos \nu\phi_0}{u} \sum_{m=1}^{\infty} \frac{\sin 2m\phi_0}{m^2}$$

$$+ \sum_{m=1}^{\infty} \left\{ G_{m\nu} \left[\frac{I_{m-1}(u)}{I_m(u)} - \frac{m}{u} \right] + \frac{\cos \nu\phi_0}{u} \frac{\sin 2m\phi_0}{m^2} \right\}. \tag{4-25}$$

The last sum in Eq. 4-23 can be determined as follows:

$$\sum_{n=N+1}^{\infty} \frac{\sin^2 \alpha_n d}{n^3} = \frac{1}{2} \int_0^{2\pi d/h} f(\theta) d\theta - \sum_{n=1}^{N} \frac{\sin^2 \alpha_n d}{n^3} \quad , \tag{4-26}$$

where f is the Clausen's integral stated in Eq. 4-10.

V. NUMERICAL RESULTS

In determining the field inside the cavity with the wire absent, the series representation of the aperture field in Eq. 2-3 is truncated at n = N (the series contains N + 1 terms). We must first establish the convergence of the aperture field with respect to N. The aperture fields as calculatedwith N = 0, 1, and 2 are shown in Figure 4. We notice that the aperture fields as computed by N = 1 and that by N = 2 agree reasonably at the main lobe but not so well at the side lobe. For many practical cases, the three-term expansion N = 2 is generally sufficiently accurate for computing the aperture field.

An indication of the accuracy of the field $\overline{E}$ inside the cavity is how well does $\overline{E}$ satisfy the boundary condition on the cavity wall (including the aperture). In Figure 5, E_z as computed from Eq. 2-26 is plotted as a function of ϕ. In the aperture defined by $|\phi| \leq 57.29^{\circ}$, the calculated E_z agrees extremely well with the two-term expansion of the aperature field calculated from Eq. 2-3. It drops to less than 0.01% of the aperture field on the wall where E_z should be ideally zero. Also shown in Figure 5 is E_z at points just behind the aperture, $\rho/a = 0.995$. The variations of E_z with respect to z at $\rho/a = 0.0$, 0.5, and 0.8 are sketched in Figure 6. As a function of decreasing (ρ/a), E_z decreases rapidly from its value in the aperture, while it increases at an even faster rate from zero on the cavity wall toward the center of the cavity. These features are illustrated in Figure 7 where E_z is plotted as a function of ρ at $z = 0.0$ and $z/h = 0.3$.

Part B of the problem is to compute the current induced on the wire inside the cavity. As mentioned in previous sections, the simple formula

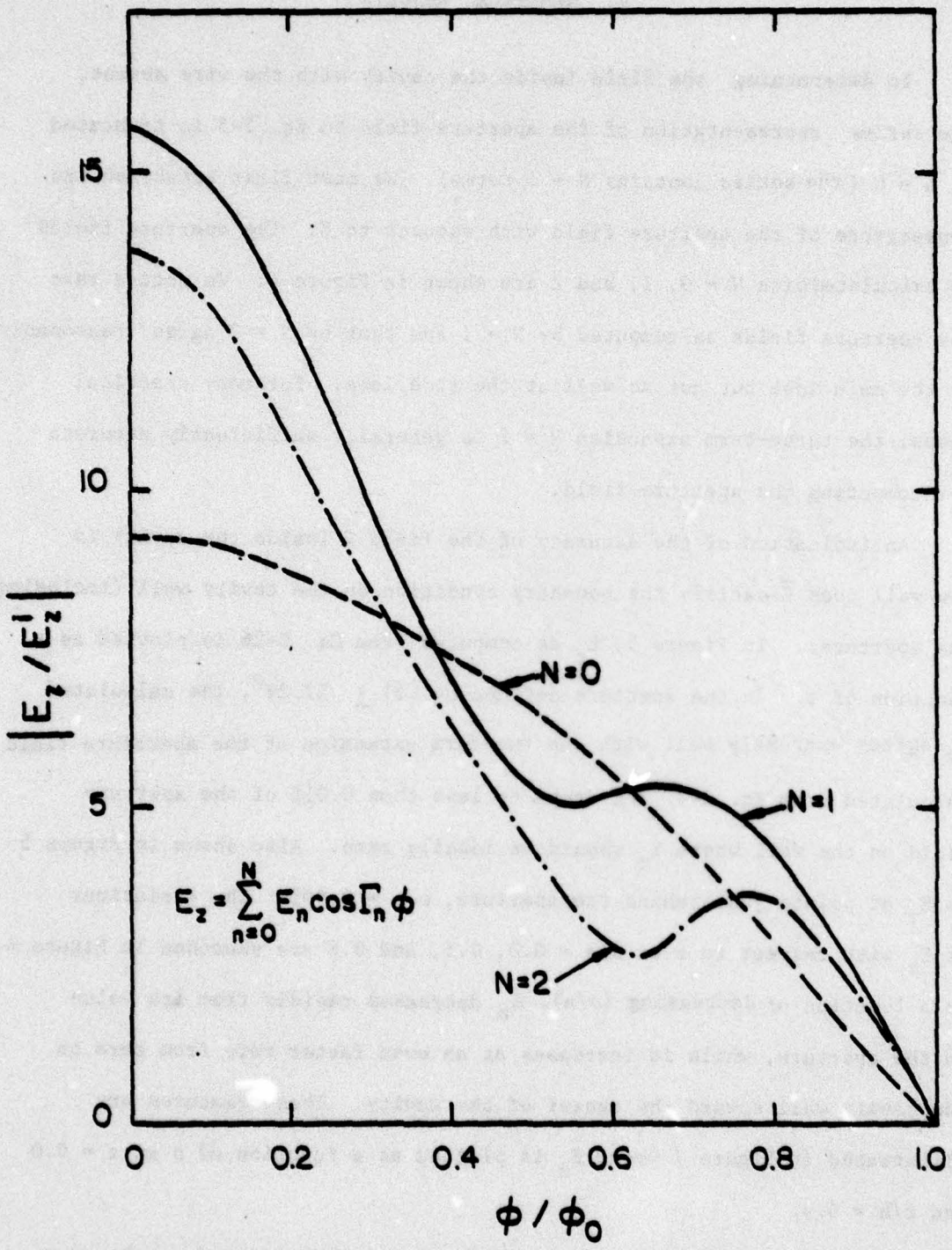

Figure 4. E_z in the aperture as a function of ϕ with N as a parameter. The input data are a = 0.3λ, c = 0.3λ, d = 0.015λ, h = 0.6λ.

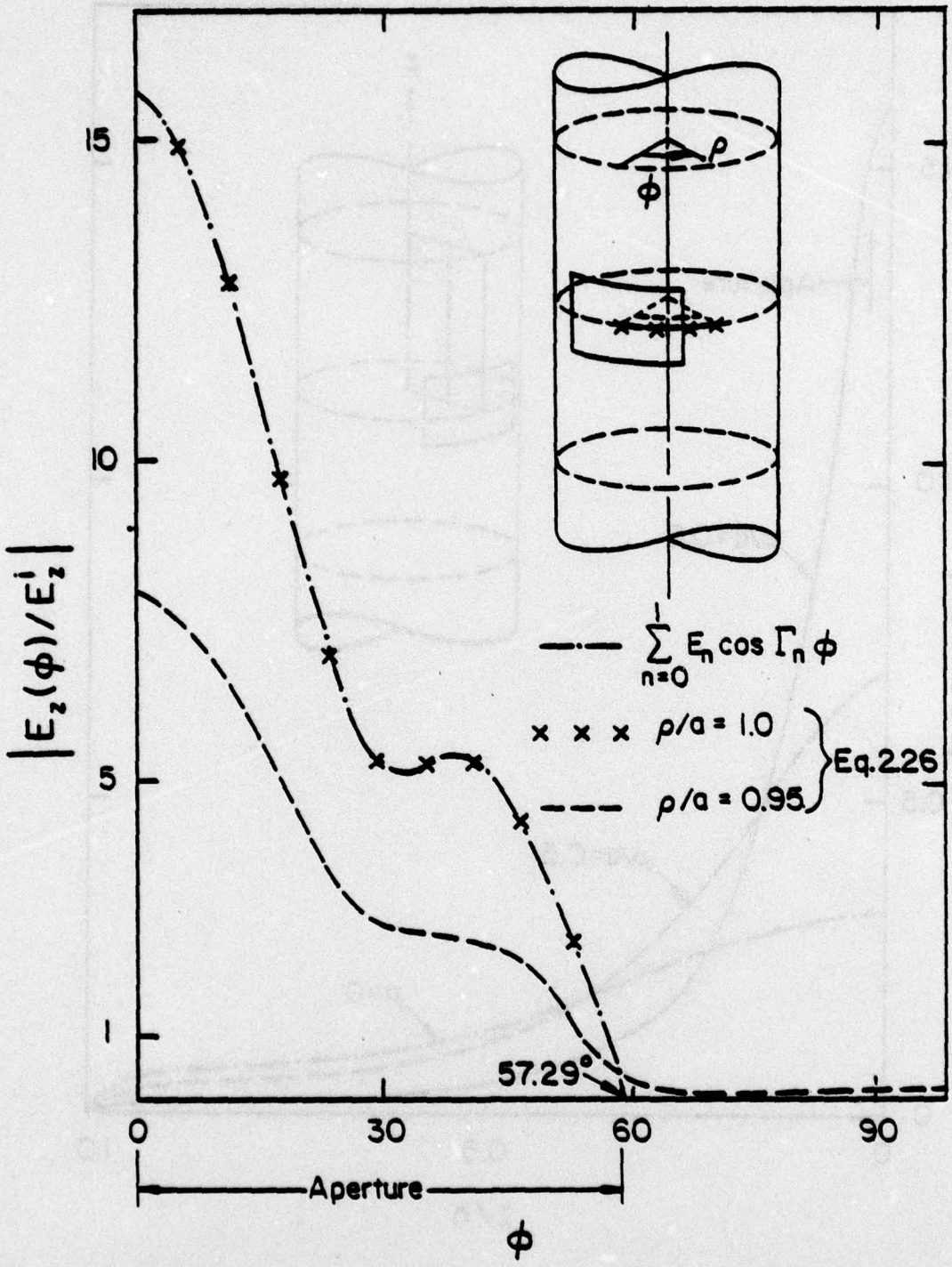

Figure 5. E_z inside the cavity as a function of ϕ with (ρ/a) as a parameter. The input data are: $a = 0.3\lambda$, $c = 0.3\lambda$, $d = 0.015\lambda$, $h = 0.6\lambda$, $\phi_0 = 1$.

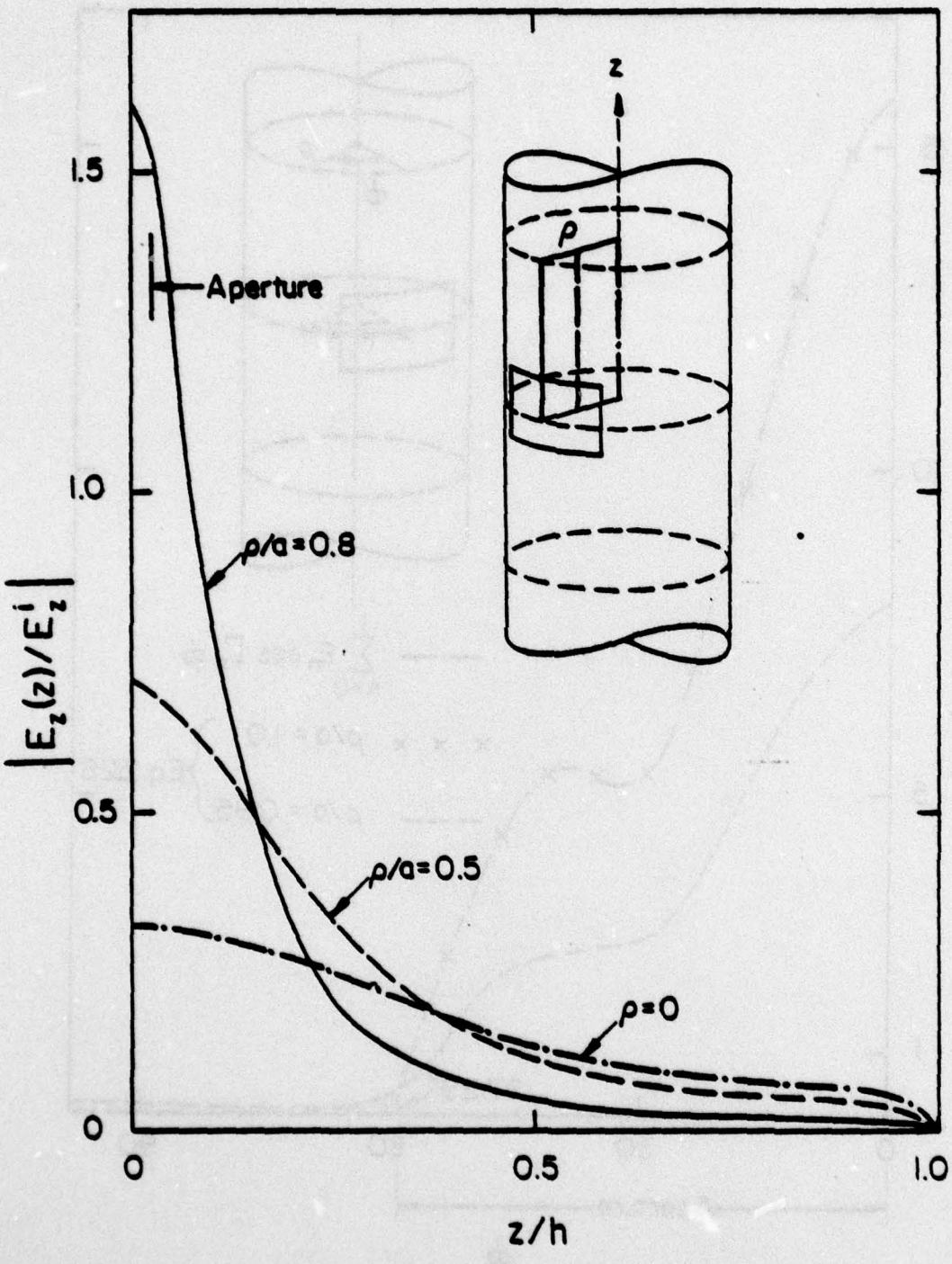

Figure 6. E_z inside the cavity as a function of z with (ρ/a) as a parameter. The input data are a = 0.3λ, c = 0.3λ, d = 0.015λ, h = 0.6λ, ϕ = 0.

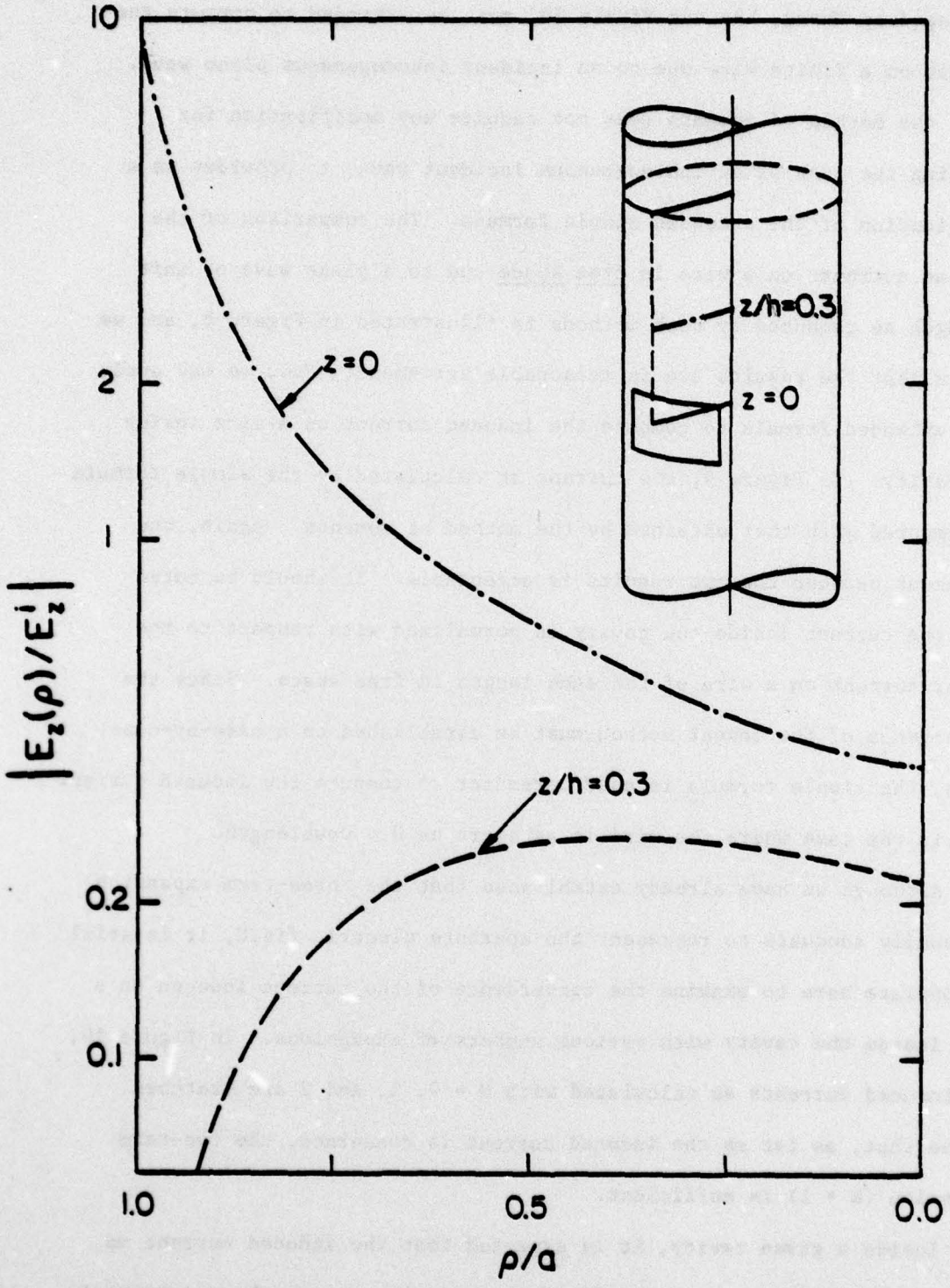

Figure 7. E_z inside the cavity as a function of ρ with (z/h) as a parameter. The input data are: a = 0.3λ, c = 0.3λ, d = 0.015λ, h = 0.6λ.

developed by Chang, Lee and Rispin [8] must be extended to compute the current on a finite wire due to an incident inhomogeneous plane wave. Since the method of moments does not require any modification for handling the case of an inhomogeneous incident wave, it provides us a verification of the extended simple formula. The comparison of the induced currents on a wire in free space due to a plane wave of unit strength as computed by both methods is illustrated in Figure 8, and we notice that the results are in reasonable agreement. Now, we may apply this extended formula to compute the induced current on a wire inside the cavity. In Figure 9, the current as calculated by the simple formula is compared with that obtained by the method of moments. Again, the agreement between the two results is acceptable. It should be noted that the current inside the cavity is normalized with respect to the center current on a wire of the same length in free space. Since the convergence of the moment method must be established on a case-by-case basis, the simple formula is used hereafter to compute the induced current even in the case where the wire is as short as 0.4 wavelength.

Although we have already established that the three-term expansion is usually adequate to represent the aperture electric field, it is still appropriate here to examine the convergence of the current induced on a wire inside the cavity with various numbers of expansions. In Figure 10, the induced currents as calculated with N = 0, 1, and 2 are sketched. We see that, as far as the induced current is concerned, the two-term expansion (N = 1) is sufficient.

Inside a given cavity, it is expected that the induced current on a given wire with its position fixed would increase with the enlargement

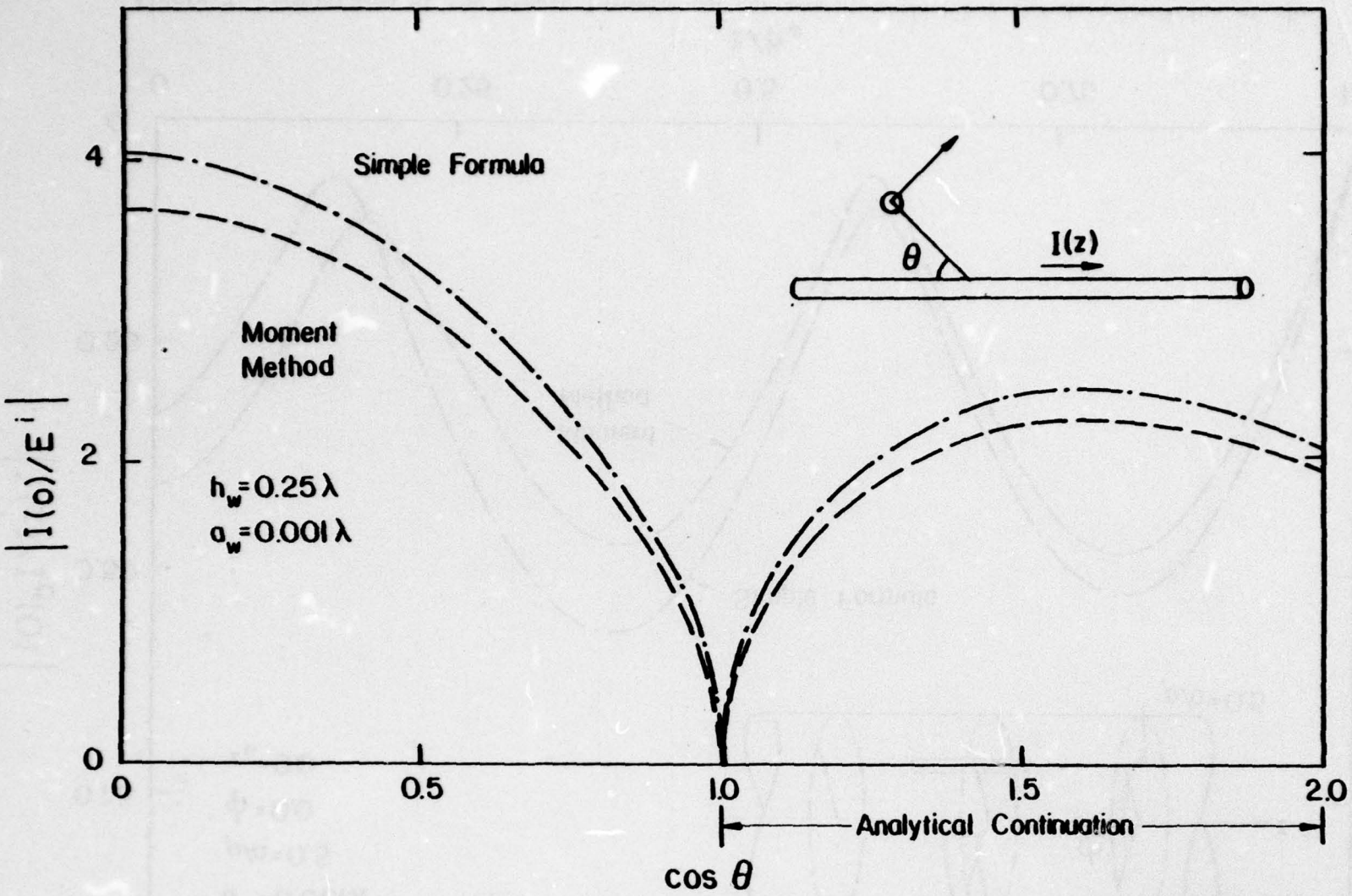

Figure 8. Comparison of the simple formula and the moment method for the determination of the current induced at the center of a cylinder in free space as a function of the angle of incidence θ (real and imaginary).

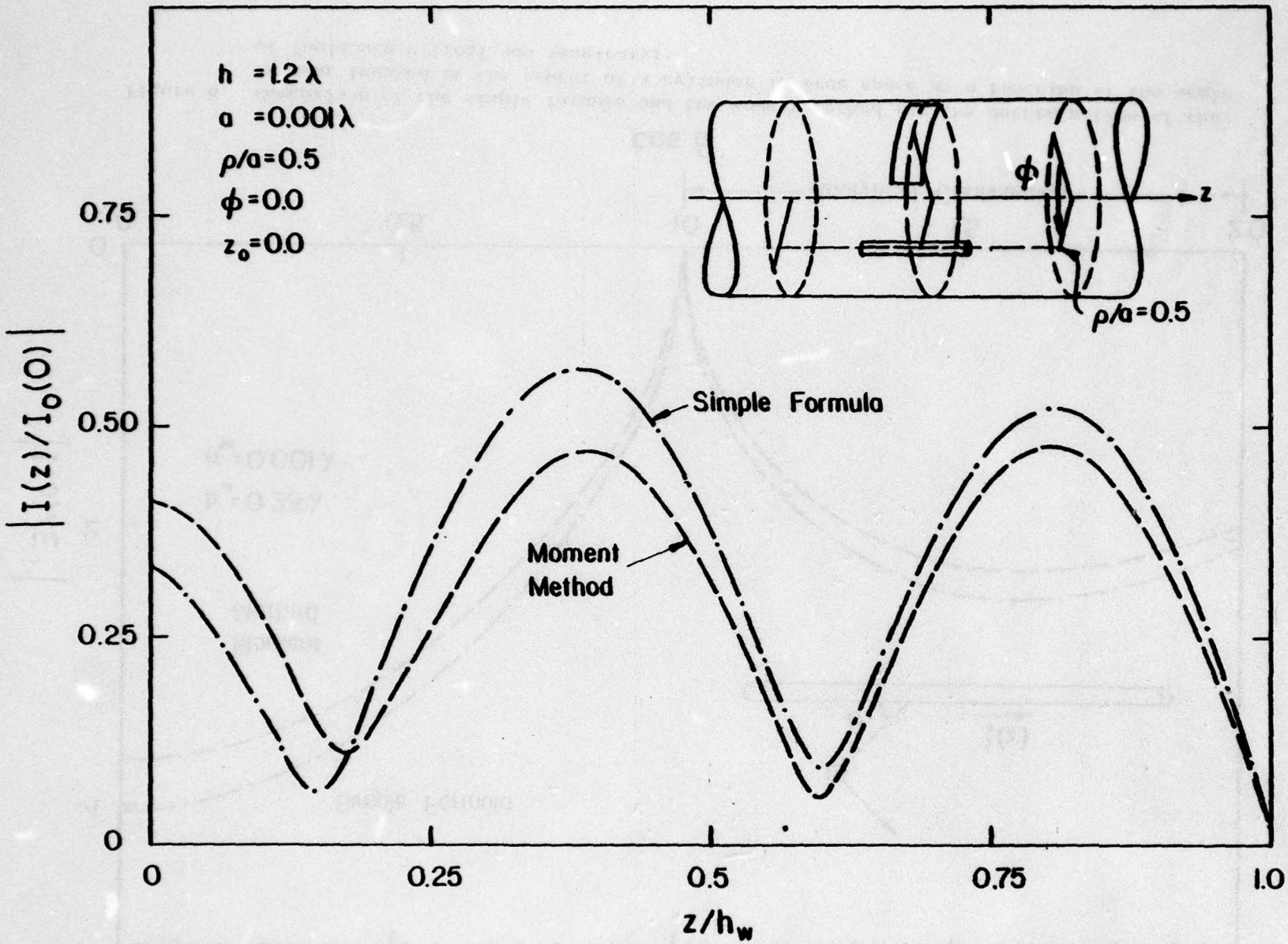

Figure 9. Comparison of the simple formula and the moment method for the determination of the induced current distribution on a wire inside the cavity. The input data are: a = 0.3λ, θ = 0.3λ, d = 0.015λ, h = 0.6λ.

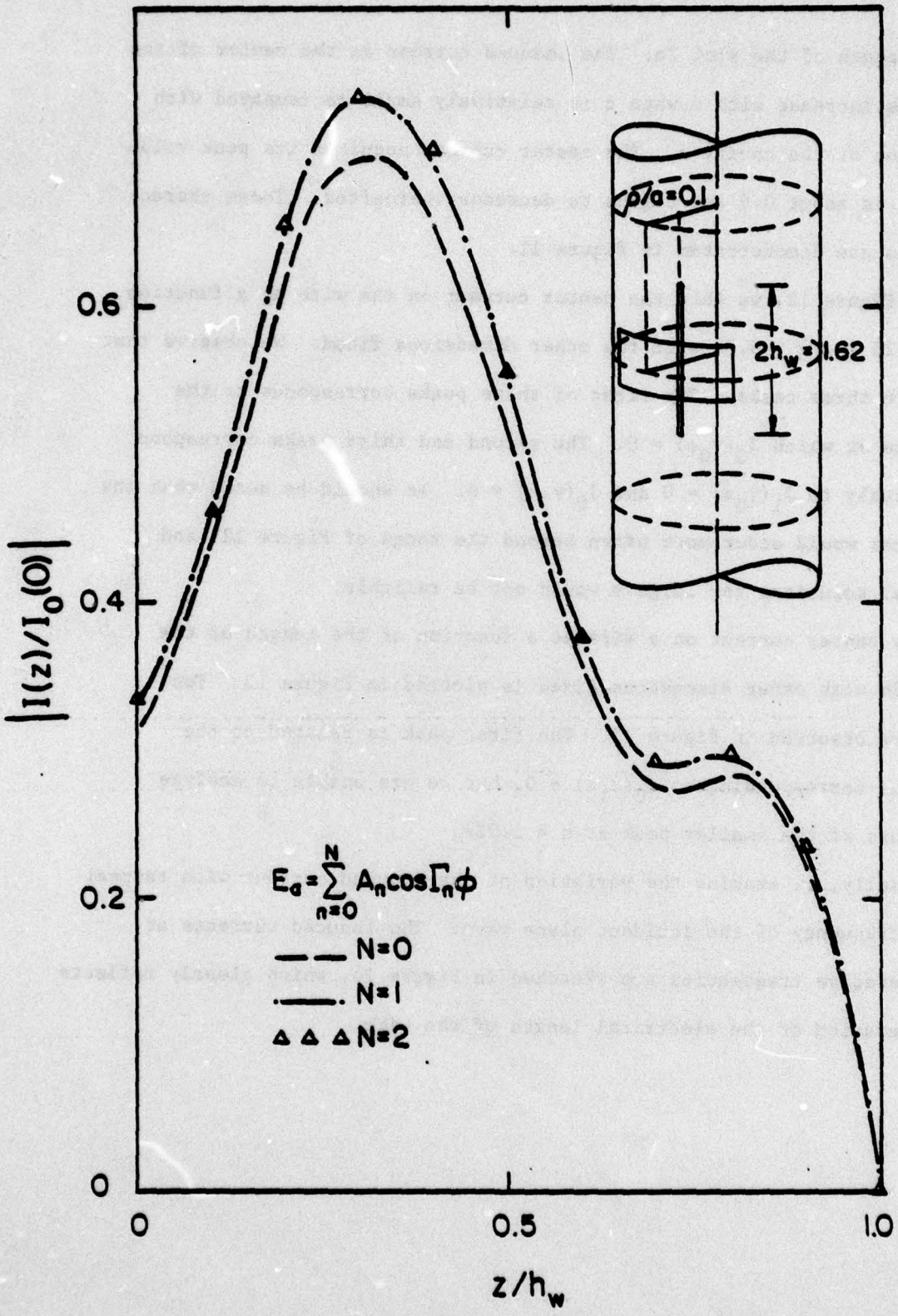

Figure 10. Induced current on a wire inside the cavity as a function of z with N as a parameter. The input data are: a = 1.0λ, c = 0.6λ, d = 0.015λ, h = 2.2λ.

of the length of the slot 2c. The induced current at the center of the wire does increase with c when c is relatively small as compared with the radius of the cavity a. The center current acquires its peak value when c/a is about 0.9 and begins to decrease thereafter. These characteristics are demonstrated in Figure 11.

In Figure 12, we show the center current on the wire as a function of a, $0.25 \leq a/\lambda \leq 0.8$, with the other dimensions fixed. We observe that there are three peaks. The first of these peaks corresponds to the resonance at which $J_0(\gamma_0 a) = 0$. The second and third peaks correspond respectively to $J_1(\gamma_0 a) = 0$ and $J_0(\gamma_1 a) = 0$. It should be noted that the resonances would occur more often beyond the range of Figure 12, and numerical solutions for large a would not be reliable.

The center current on a wire as a function of the length of the cavity 2h with other dimensions fixed is plotted in Figure 13. Two peaks are observed in Figure 13. The first peak is related to the resonance corresponding to $J_0(\gamma_1 a) = 0$, but we are unable to analyze the nature of the smaller peak at $h = 1.02\lambda$.

Finally, we examine the variation of the induced current with respect to the frequency of the incident plane wave. The induced currents at representative frequencies are sketched in Figure 14, which clearly reflects the alteration of the electrical length of the wire.

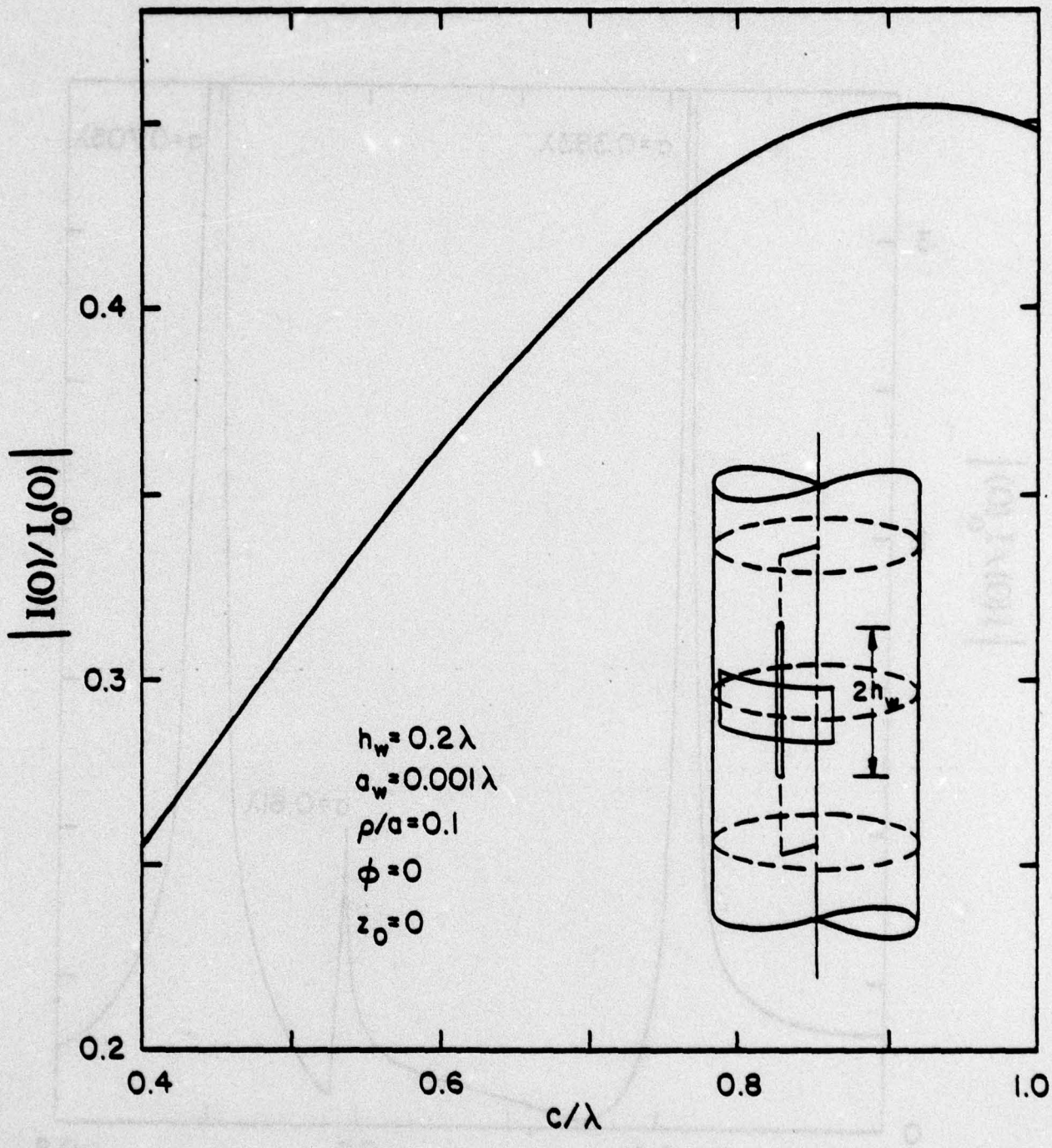

Figure 11. Induced current at the center of the wire inside the cavity as a function of slot length 2c. The input data are: a = 1, d = 0.015, h = 2.2, freq. = 0.3.

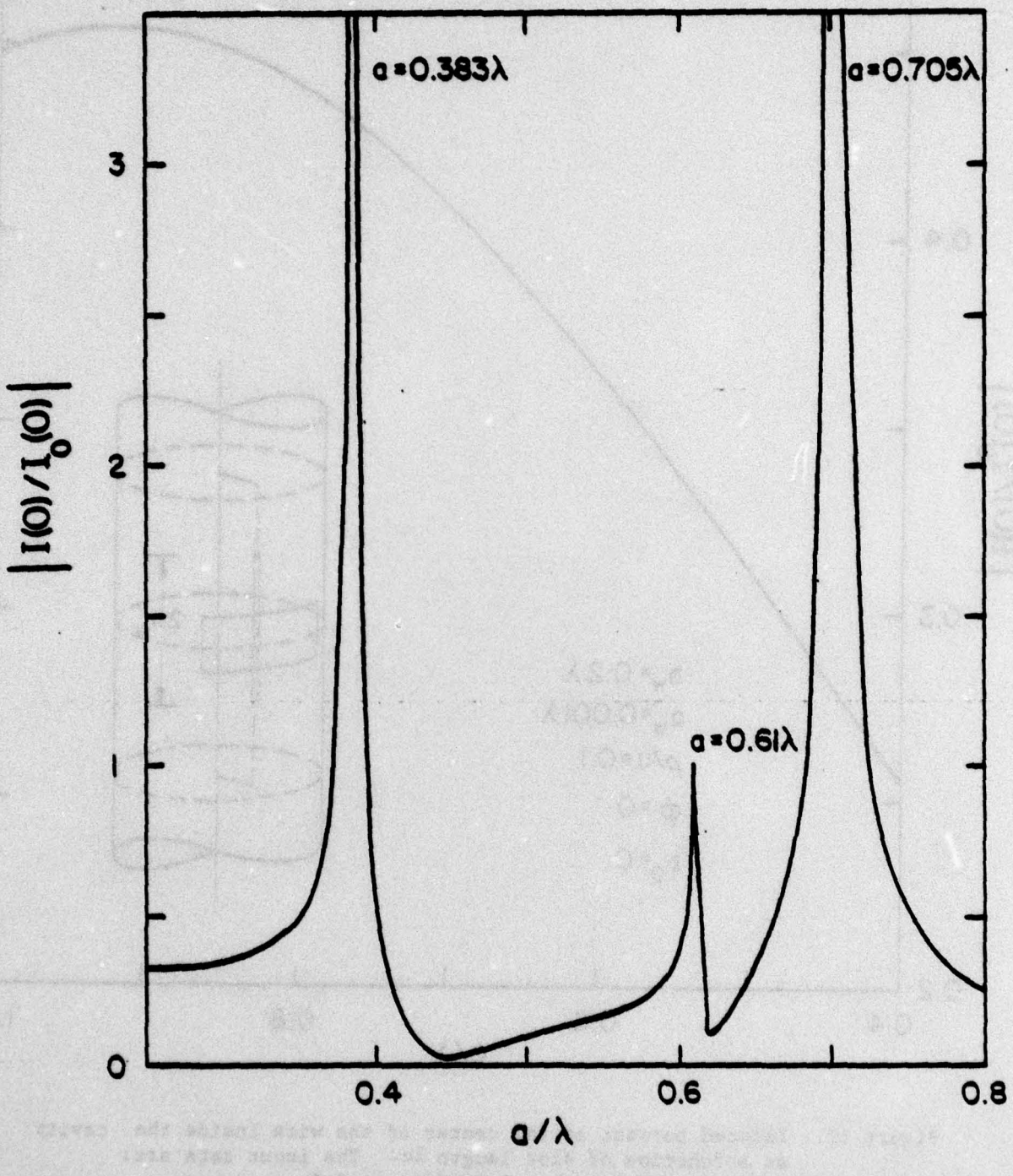

Figure 12. Induced current at the center of the wire inside the cavity as a function of cylinder radius a. The input data are: $c = 0.3\lambda$, $d = 0.015\lambda$, $h = 0.6\lambda$, $h_w = 0.2\lambda$, $\rho/a = 0.1$.

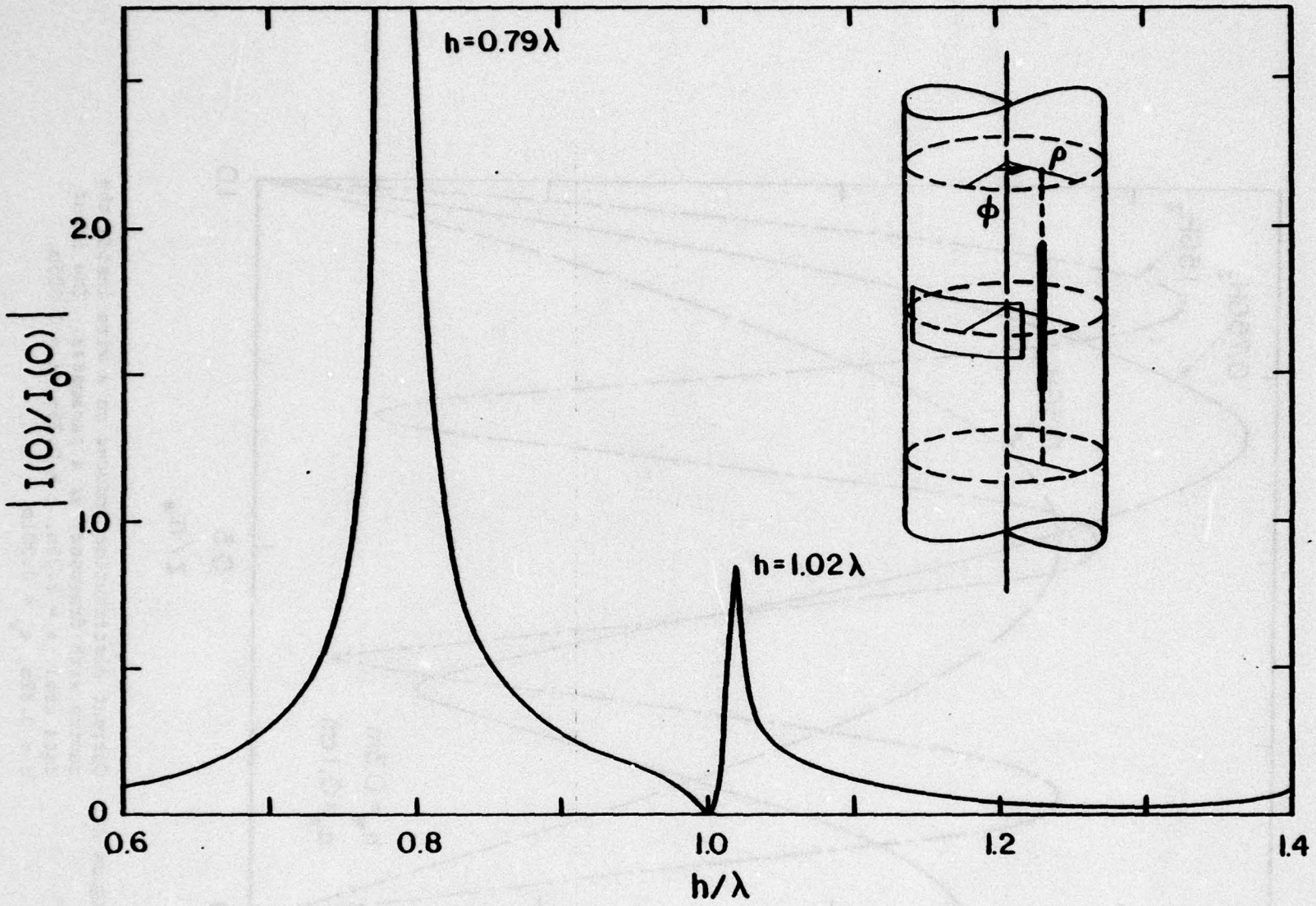

Figure 13. Induced current at the center of the wire inside the cavity as a function of cavity length 2h. The input data are: $a = 0.5\lambda$, $c = 0.3\lambda$, $d = 0.015\lambda$, $h_w = 0.2\lambda$, $a_w = 0.001\lambda$, $\rho/a = 0.1$.

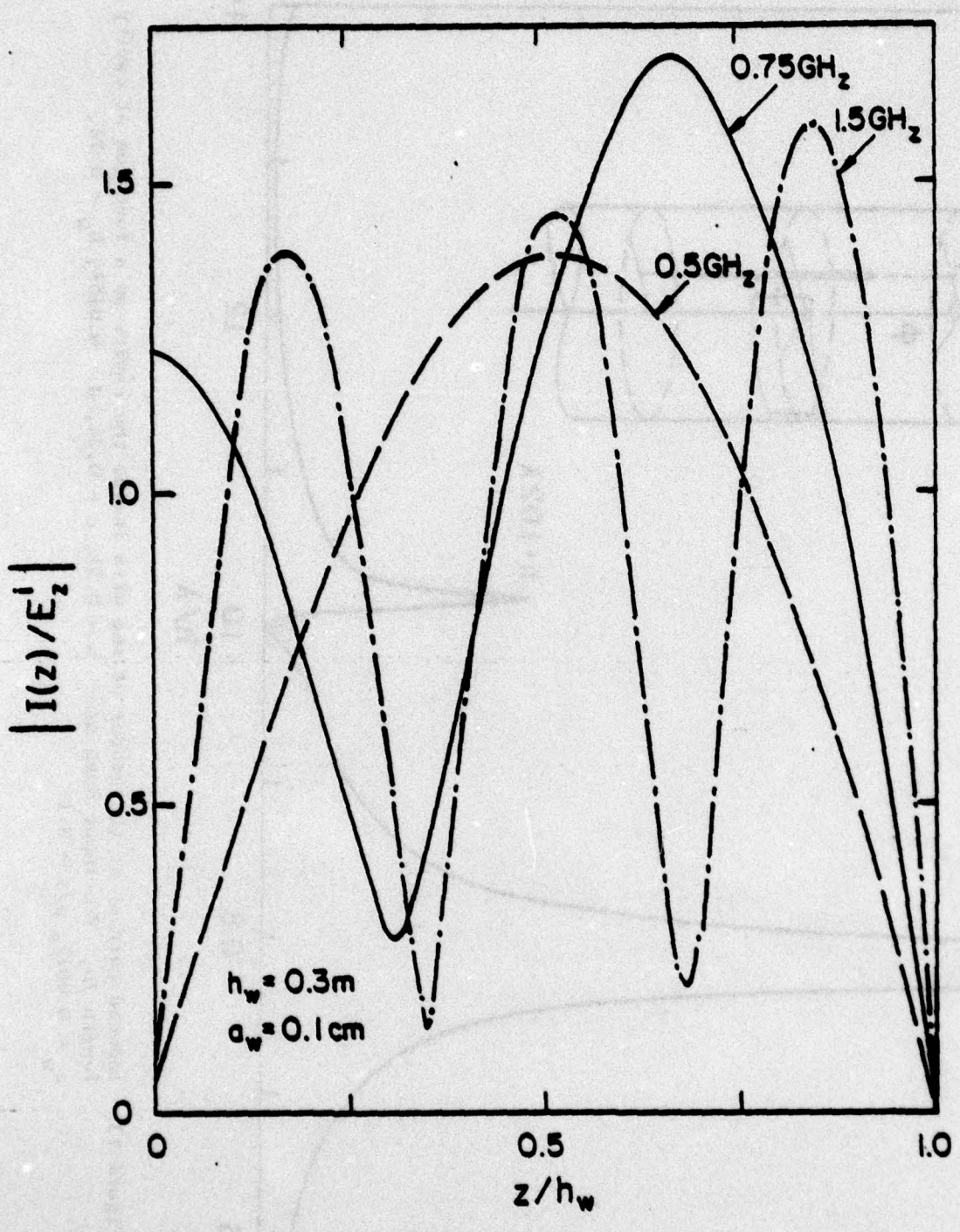

Figure 14. Current distribution induced on a wire inside the cavity with frequency as a parameter. The input data are: a = 0.35m, c = 0.25m, d = 0.005m, h = 0.82m, a_w = 0.001m.

REFERENCES

[1] A. Sommerfeld, Partial Differential Equations in Physics, New York, Academic Press, 1949, pp. 29, 159.

[2] Silvers and Saunders, "The External Field Produced by a Slot in an Infinite Circular Cylinder," J. Appl. Phys., Vol. 21, 5, pp. 153-158, Feb., 1950.

[3] R. Barakat and E. Levin, "Diffraction of a Plane EM Wave by a Perfectly Conducting Cylindrical Lamina," J. Opt. Soc. Amer., Vol. 54, 9, pp. 1089-1094, 1964.

[4] R. F. Wallenberg, "Radiation from Aperture in Conducting Cylinders of Arbitrary Cross Section," IEEE Trans. Antennas Propagat., Vol. AP-17, No. 1, pp. 56-62, 1974.

[5] L. L. Bailin and R. J. Spellmire, "Convergent Representations for the Radiation Fields from Slots in Large Circular Cylinders," IRE Trans. Antennas Propagat., Vol. AP-5, pp. 374-383, 1957.

[6] S. Safavi-Naini, "Diffraction of Electromagnetic Waves by a Slotted Circular Cylinder," M.S. Thesis, University of Illinois, Urbana, 1976.

[7] S. Safavi-Naini, S. W. Lee, and R. Mittra, "Transmission of an EM Wave through the Aperture of a Cylindrical Cavity," Electromagnetic Lab. Technical Report No. 76-1, University of Illinois, Urbana, 1976.

[8] S. Safavi-Naini, S. W. Lee, and R. Mittra, "Transmission of EM Wave through the Aperture of a Cylindrical Cavity," IEEE Trans. Electromagn. Comput., Vol. EMC-19, pp. 74-81, 1977.

[9] R. F. Harrington, Field Computation by Moment Methods, Macmillan, New York, 1968, pp. 7, 178.

[10] C. M. Butler, "Evaluation of Potential Integral at Singularity of Exact Kernel in Thin-Wire Calculations," IEEE Trans. Antennas Propagat., Vol. AP-23, pp. 293-294, March, 1975.

[11] D. C. Chang, S. W. Lee, and L. Rispin, "Simple Expressions for Current on a Thin Cylindrical Receiving Antenna," Scientific Report No. 20, University of Colorado, Dec., 1976.

[12] D. C. Chang, S. W. Lee, and L. Rispin, "Simple Formula for Current on a Cylindrical Receiving Antenna," Electromagnetic Lab. Technical Report No. 77-10, University of Illinois, May, 1977; to appear in IEEE Trans. Antennas Propagat., 1978.

[13] R. F. Harrington, Time-Harmonic Electromagnetic Fields, McGraw Hill, New York, 1961, p. 200.

[14] M. Abramowitz and I. Segun, Handbook of Mathematical Functions, Dover, New York, p. 1005.

[15] Ibid, p. 232.